KTH Electrical Engineering

A Stochastic Control Approach to Include Transfer Limits in Power System Operation

MAGNUS PERNINGE

Doctoral Thesis
Stockholm, Sweden 2011

TRITA-EE
ISSN
ISBN 978-91-7415-308-8

KTH School of Electrical Engineering
SE-100 44 Stockholm
SWEDEN

Akademisk avhandling som med tillstånd av Kungl Tekniska högskolan framlägges till offentlig granskning för avläggande av teknologie doktorsexamen måndag den 7 november 2011 klockan 10.00 i F3, Lindstedtsvägen 26, Kungl Tekniska högskolan, Stockholm.

Tryck: Universitetsservice US AB

Abstract

The main function of the power grid is to transfer electric energy from generating facilities to consumers. To have a reliable and economical supply of electricity, large amounts of electric energy often have to be transferred over long distances.

The transmission system has a limited capacity to transfer electric power, called the *transfer capacity*. Severe system failures may follow if the transfer capacity is reached during operation.

Due to uncertainties, such as the random failure of system components, the transfer capacity for the near future is not readily determinable. Also, due to market principles, and reaction times and ramp rates of production facilities, power flow control is not fully flexible. Therefore, a *transfer limit*, which is below the transfer capacity, is decided and preventative actions are taken when the transfer reaches this limit.

In this thesis an approach to deciding an optimal strategy for power flow control through activation of regulating bids on the regulating power market is outlined. This approach leads to an optimal definition of transfer limits as the boundary between the domain where no bid should be activated and the domains where bids should be activated. The approach is based on weighing the expected cost from system failures against the production cost. This leads to a stochastic impulse control problem for a Markov process in continuous time.

The proposed method is a novel approach to decide transfer limits in power system operation. The method is tested in a case study on the IEEE 39 bus system, that shows promising results.

In addition to deciding optimal transfer limits, it is also investigated how the transfer capacity can be enhanced by controlling components in the power system to increase stability.

Keywords: Frequency control, power regulating market, power system operation, power system security, stochastic impulse control, transfer capacity, transfer limit.

Acknowledgements

First, I would like to thank Lennart Söder for employing me and supervising me throughout the project. A special thanks to Valerijs Knazkins and Mikael Amelin for their guidance during the early stages of the project, and to Filip Lindskog for interesting discussions on applied probability and stochastic processes. I would also like to thank Camille Hamon and Mikael Amelin for their valuable comments on the thesis, and Katherine Elkington for help with the English language.

Moreover, I would like to thank the Center of Excellence in Electric Power Engineering (EKC^2) at Royal Institute of Technology for their financial support of this project.

Finally, I would like to thank all my fellow PhD students at Electric Power Systems, KTH.

Dissertation

This doctoral thesis includes an introduction to power system operation and transmission limits. The thesis is based on the material in 10 appended articles. These are:

Article I

M. Perninge, V. Knazkins, M. Amelin and L. Söder, "Modeling the electric power consumption in a multi-area system", *European Transactions on Electric Power*, 2011, Vol. 21(1), pp. 413-423.

Article II

M. Perninge, and L. Söder, "Analysis of transfer-limit induced power system security by Markov chain Monte Carlo simulation", *To appear in European Transactions on Electric Power*, 2011.

Article III

M. Perninge, and L. Söder, "Risk estimation of the distance to voltage instability using a second order approximation of the saddle-node bifurcation surface", *Electric Power System Research*, 2011, Vol. 81(2), pp. 625-635.

Article IV

M. Perninge, and L. Söder, "On the validity of local approximations of the power system loadability surface", *To appear in IEEE Transaction on Power Systems*, 2011.

Article V

M. Perninge, F. Lindskog and L. Söder, "Importance Sampling of Injected Powers for Electric Power System Security Analysis", *To appear in IEEE Transactions on Power Systems*, 2011.

Article VI

M. Perninge, and L. Söder, "Optimal activation of regulating bids to handle bottlenecks in power system operation", *Submitted to Electric Power System Research*, 2011.

Article VII

M. Perninge, and L. Söder, "A Stochastic Control Approach to Manage Operational Risk in Power Systems", *Submitted to IEEE Transactions on Power Systems*, 2011.

Article VIII

M. Perninge, and L. Söder, "Optimal activation of regulating bids in power system operation", *Submitted to Mathematical Methods of Operations Research*, 2011.

Article IX

M. Perninge, and L. Söder, "Optimal distribution of primary control participation with respect to voltage stability", *Electric Power Systems Research*, 2010, Vol. 80(11), pp. 1357-1363.

Article X

R. Eriksson, M. Perninge, and L. Söder, "Transfer capacity enhancement by adaptive coordinated control of HVDC-links based on forecasted load paths", *European Transactions on Electric Power*, 2011, Vol. 21(3), pp. 1455-1466.

Division of work between the authors

Article I
M. Perninge drew up the outline, carried out the work and wrote this article under the supervision of V. Knazkins, M. Amelin and L. Söder.

Articles II, III, IV, VI, VII and VIII
M. Perninge drew up the outline, carried out the work and wrote these articles under the supervision of L. Söder.

Article V
M. Perninge drew up the outline, carried out the work and wrote this article under the supervision of F. Lindskog and L. Söder.

Article IX
M. Perninge drew up the outline, carried out the work and wrote this article under the supervision of L. Söder. Although not listed as one of the authors we owe gratitude to V. Knazkins for providing insightful comments to this article.

Article X
R. Eriksson and M. Perninge jointly drew up the outline, carried out the work and wrote this article under the supervision of L. Söder.

The PhD-project

This doctoral thesis is written as the final part of the PhD-project "Regulation for Efficient use of Transmission Systems on Electricity Markets". The financial support of this project was provided by the Center of Excellence in Electric Power Engineering (EKC^2) at Royal Institute of Technology. Other publications from to this project, which have not been included in the thesis, are [1–11].

Contents

Chapter 1

Introduction

This chapter introduces the topic of this thesis, defines the scope and objective and presents the scientific contributions.

The main function of the power grid is to transfer electric energy from generating facilities to consumers. To have a reliable and economical supply of electricity large amounts of electric energy often have to be transferred over long distances. Examples include when a major part of of the electricity production comes from renewable energy sources, such as hydro- and wind power, where the generating facilities often are located at a substantial distance from the regions where the main consumption is.

The transmission system has a limited capacity to transfer electric power, called the *transfer capacity* [12]. Severe system failures may follow if the transfer capacity is reached during operation.

Due to uncertainties, such as the random failure of system components, the transfer capacity for the near future is not readily determinable. Instead a *transfer limit*, which is below the transfer capacity, is decided and preventative actions are taken when the transfer reaches this limit.

Transfer limits are important aspects in power system operation. Planners need to be able to estimate how much energy that can be traded between different areas of the system and the system operators need to know how to operate the system.

When deciding on adequate transfer limits there is a conflict of interest. On the one hand it is economically desirable to transfer large amounts of electric power through the grid. On the other hand it is important to run the system in a safe and secure manner. The trade-off between transfer and security can be resembled with the functions sketched in Figure 1.1. Increasing the transfer will reduce the cost of production, but increase the part of the expected cost for society coming from system failures.

Above it was mentioned that random failures of system components is one aspect that influences the size of the transfer capacity, which in turn influences the

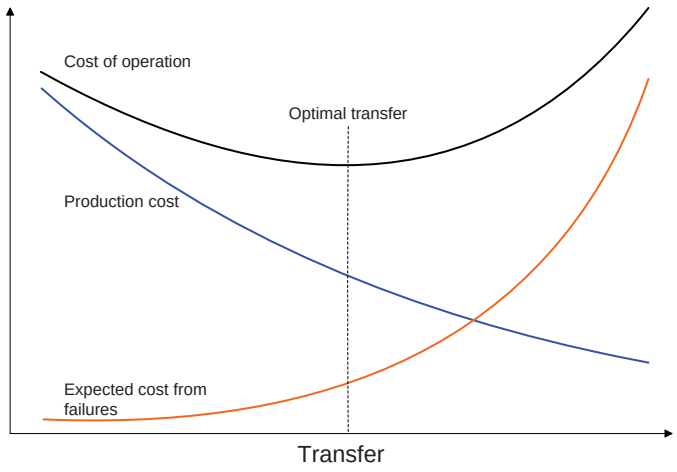

Figure 1.1: The trade-off between transfer and security.

size of adequate transfer limits. Another aspect is the random fluctuation of power consumption. Since there must at all times be a balance between production and consumption, production is forced to change to follow the aggregate load fluctuations. This is in part done automatically by letting a number of power plants in the system have their production depend on the frequency [13]. The fact that some power plants change their production automatically to maintain the balance between production and consumption in the system, means that fluctuations are in general not balanced locally. This will introduce an uncertainty in the flows through the grid.

To limit the strain on the system, observable system variables, such as the flows through certain "critical" transmission corridors, are monitored. When these "observables" reach a pre-decided level, actions are taken to reduce the strain on the system and maintain secure operation. The actions taken constitute what is known as the *tertiary control* [14]. The tertiary control is manually operated in the sense that the system operator contacts a producer and asks him to change the production in one of his power plants, or asks a consumer to change his consumption. We call the spare capacity available for tertiary control *tertiary reserves*. In a deregulated market the tertiary reserves are provided through a market called the *regulating market* [15]. Bids handed in to the this market are called *regulating bids*.

The tertiary control is used to balance the system frequency in a cost optimal way and to handle bottlenecks. When used to balance frequency the cheapest available bid can be used. However, when used to handle bottlenecks in the transmission grid the geographic positions of the reserves have to be considered and the cost order of the bids might have to be sidestepped. This will lead to a higher production cost than if the bottleneck was not present.

In many systems there is a generation control that acts slower than the primary control and faster than the tertiary control. This generation control system is called *secondary control*. Besides from controlling the balance between production and consumption, the secondary control can also be used to control the power transfer on certain tie-lines. It should be emphasized that we in this thesis will not consider optimization of the secondary control.

1.1 Objectives

The objective of this thesis is to investigate how to manage the operation of the system to optimally balance the benefit of power transfer against system security. This objective leads to different questions that have to be answered. The questions that we will try to answer in this thesis are the following:

Q1 What is the risk of system failure given a certain level of power transfer?

Q2 How do we activate regulating bids in order to minimize the expected cost of operation?

Q3 How can we increase the transfer capacity by controlling available system equipment?

To provide an answer to Q1 there are certain issues that need to be considered. First we need to analyze the physical constraints limiting the transfer capacity. The transfer capacity will depend on, for example, the distribution of the load amongst the nodes of the system [16], limitations in generating units [17] and the risk of outages in system equipment [18]. In addition to this we need to analyze the restrictions caused by the lack of flexibility when controlling the power flows through the regulating market.

In Q2, when we say expected cost of operation we mean the expected net cost from the activation of regulating bids, plus the expected cost from system failures. There is an obvious connection between Q1 and Q2. In order to optimize the activation of regulating bids we need to know the expected cost at each specific level of system stress, which is the sum of the costs of each type of disturbance that can occur times the risk of the disturbance.

One way of optimizing the utilization of the power grid is to use adequate transfer limits, another way is to try to enhance the transfer capacity by making better use of the available systems components. Therefor, Q3 is also an important question in power system operation.

To summarize the objective in terms of the curves in Figure 1.1, the answer to Q1 provides means of finding the (red) curve representing the expected cost from system failure, the answer to Q2 is that we should run the system to minimize the value of the sum of the two curves, and Q3 concerns how to push the expected operation cost curve to the right.

1.2 Scientific contributions

Q1–Q3 are fundamental questions in the operation of power systems, and providing complete answers to all of them is out of the scope of a doctoral thesis. Therefore, some narrowing of the objectives had to be adopted, when attacking the problems.

The scientific contributions of the work presented in this thesis can be divided between the three different questions posed in the previous section as follows.

Q1

Here, we have focused on long-term voltage stability [17], rendering the loadability limit surface as physical limit. We analyze what impact lack of flexibility in the tertiary control will have on the risk of system failure.

This required development of a stochastic model of the power consumption. Also, we provide means of analyzing approximations of the loadability limit surface, *i.e.* the surface made up of all points of maximal loadability.

Q2

We develop a method for estimating the optimal strategy for activation of regulating bids. The method is based on transforming the risk of system failure from Q1, into a monetary value. Then impulse control is used to optimize the activation of regulating bids in order to minimize the expected cost of operation. Here, each impulse represents the activation of a regulating bid.

The resulting control will take the form of a partition of the space where the observables live into a continuation region and a number of activation regions. The continuation region is defined so that it is optimal to activate a regulating bid once the observables leave this domain. The boundary of the continuation region can thus be seen as a type of transfer limit surface.

Important aspects here are the delays in reaction of the actors on the regulating market and the ramp rates of their power plants. Inclusion of these gives the impulse control problem delayed reaction. This required development of new numerical stochastic control schemes.

The developments here are fundamentally different from previous research in the area of power system operation where the use of a security criteria, for example the $(N-1)$–criteria, has been the main tool to define transfer limits [18].

Q3

Another way of using the system in a more efficient way is to use the existing power system components more efficiently to increase the transfer capacity. Here adaptive control and coordination of the control of different system components are the main measures of increasing the transfer capacity.

The objective of each such control scheme is to improve the stability properties of the system.

We propose two methods for enhancing the transfer capacity. The first method is based on optimizing the distribution of the primary control gain to maximize the distance of the present operating point to the saddle-node bifurcation surface. This means that we distribute the automatic control resources to avoid steady-state voltage instability.

The second approach assumes that the system contains several HVDC-links and tunes the power modulation gain of these links to enhance the small signal stability properties of the system.

List of main contributions

To summarize, the following are the main contributions of the work presented in this thesis:

i) A stochastic model of the consumption in a multi-area power system is developed (Article I).

ii) A method for generating samples of injected power given the power flows through a number of transmission corridors is developed (Article II).

iii) Two methods for estimating the probability of voltage collapse within a certain time period is proposed. The first is an analytical method (Article III) while the second method is based on Monte Carlo simulation (Article V).

iv) A method for investigating the validity of local approximations of the loadability limit surface is developed (Article IV)

v) A control strategy for optimizing the activation of one regulating bid, based on the flow through one transmission corridor is proposed (Article VI).

vi) A Monte Carlo based method for finding the control strategy that optimizes the activation of several regulating bids, based on a number of system observables, is proposed (Articles VII and VIII).

vii) A method for optimizing the distribution of the primary control reserve with respect to the distance to voltage collapse is developed (Article IX).

viii) A method for coordinating the control of several HVDC-links is suggested (Article X).

1.3 Thesis outline

The outline of the thesis is based on a partition into the three parts. One part for each question to be answered. First, in the next chapter a deeper background is

given. Then follows three chapters each dedicated to answering one of the three different questions Q1, Q2 and Q3. In the last chapter before the appended articles some conclusions that can be drawn from the work are given and possible future work is discussed.

The chapters can be summarized as follows:

Chapter 2 In this chapter background to the thesis area is given. We give a short introduction to how electricity markets work and discuss implications of lack of flexibility in the generation control. This chapter also contains a summary of the standard for deciding transmission limits today. As an example we consider the power system in Sweden which is a part of the Nordic power system.

Chapter 3 This chapter deals with the evaluation of the risk induced by keeping a certain transfer level. The main challenge we face here is that, due to lack of flexibility in the generation control, we have to estimate the risk of system failure within a short time following any contingency. Short introductions to Articles I–V are given in this chapter.

Chapter 4 In this chapter we present an overview of our stochastic control based approach to power system operation which is the main contribution of the thesis. We make comparisons and discuss differences to earlier research devoted to applications in mathematical finance. This chapter serves as a prelude to Articles VI–VIII. Short introductions and comments to these articles are given at the end of the chapter.

Chapter 5 In this chapter we discuss how the physical capacity to transfer electric power can be enhanced. At the end of this chapter we give short introductions to Articles IX and X.

Chapter 6 In this, the last chapter of the thesis, conclusions are drawn and guidelines for future work are outlined. We discuss how the methods presented in the appended articles can be improved and further developed to meet the increasing demand on efficient power system operation.

Chapters 3-5 are introductions to the articles.

Chapter 2

Background

In this chapter background to the thesis area is given. We give a short introduction to how electricity markets work and discuss implications of lack of flexibility in the generation control. This chapter also contains a summary of the standard for deciding transmission limits today. As an example we consider the power system in Sweden which is a part of the Nordic power system.

There are several aspects which influence the risk of system failure when keeping a certain transfer level [19].

First there are the physical constraints, these include steady-state voltage stability, thermal stability and dynamic stability. In general, serious consequences will follow if any of these constraints are violated. In addition to these constraints there are softer constraints such as limits for the allowed voltage levels.

System components will not be functional with 100% certainty at all times. There may, for example, be an outage in a generating unit or a power line. Such contingencies tend to reduce the transfer capacity.

Since disturbances are often costly we need to consider the transfer capacity also for contingency cases when determining adequate transfer limits. Even though the probability of an outage in system equipment is small.

In addition to the physical transfer capacity of the system, the control actions that the system operator can use to reduce the strain on the system are not totally flexible. There are, for example, ramp rates of all generators. The ramp rate specifies the maximal increment in power output per time unit from the generator. A power plant with a lower ramp rate is thus less flexible. Using less flexible generating units to balance the demand will require more planning and better forecasts from the system operator.

Related to the flexibility of the generating units is the variations in the net load. A highly varying net load requires more flexible balancing units or even better forecasts and more planning from the system operator. Here, net load means system load minus power produced in variable generating units. An increased use

of variable energy sources such as wind power, wave power and solar power, will introduce more uncertainty in the net load, and thus raise the requirement on the control methods used for balancing.

We start by looking what a mathematical model of the power system and the physical constraints, which define the transfer capacity, may look like.

2.1 Power system modeling

In power system analysis, the main objective is to evaluate how a number of system variables evolve over time. These variables are typically voltage magnitudes and angles at system nodes, and state variables for the generators of the system. Let $z \in \mathbb{R}^{n_z}$ be a vector representing the subset of these power system variables which are directly governed by the dynamic behavior of machines, such as the state variables of generators. Let $y \in \mathbb{R}^{n_y}$ be a vector representing the subset of these power system variables which are not directly governed by the dynamic behavior of machines, such as the voltage magnitudes and angles at the system nodes. Additional to the system variables there are a number of system parameters. These parameters can be collected into a vector $\Gamma = (u, \lambda)$, where $u \in U \subset \mathbb{R}^{n_u}$ is a vector of controllable parameters such as the set-point of generators, and $\lambda \in \mathbb{R}^{n_\lambda}$ is a vector of variable, uncontrollable, system parameters such as the loading at each node of the system.

The power system is generally modeled by a set of differential-algebraic equations [20]:

$$\dot{z} = F(z, y, \Gamma), \tag{2.1a}$$

$$0 = G(z, y, \Gamma). \tag{2.1b}$$

Here, $F : \mathbb{R}^{n_z} \times \mathbb{R}^{n_y} \times \mathbb{R}^{n_u+n_\lambda} \to \mathbb{R}^{n_z}$ is the model of generators and other dynamic equipment in the system, and $G : \mathbb{R}^{n_z} \times \mathbb{R}^{n_y} \times \mathbb{R}^{n_u+n_\lambda} \to \mathbb{R}^{n_y}$ represents the power grid.

It is important that, as the variable system parameters λ evolve over time, the system operating point $x = (z, y)$ remains within the domain of attraction of the stable operating point of the system. Additional to this there may be other constraints such as limits on line flows and voltage level at load nodes.

Crucial events where stability is threatened is when an outage in any system equipment occurs. This is generally referred to as a *contingency* and will change the structure of the functions F and G.

Physical constraints

The ability of a power system to transfer electric power from one node to another is usually limited by one of the following constraints [17, 19–21]:

Steady-state voltage stability The operating point must always be in the upper part of the nose curve. The nose curve is the nose-shaped curve showing the

relationship between the voltage at a system node and a loading parameter (see Figure 2.1).

Thermal stability To prevent overheating some of the system equipment, such as power-lines, will be disconnected if the current flowing through them becomes to large. Therefore, the electric power transfers in the system cannot be allowed to exceed some maximal value.

Voltage limits The voltages at certain nodes may have to be kept within a predefined interval.

Dynamic stability The system state must always remain within the domain of attraction of the corresponding stable operating point.

It will be assumed that violation of any of these constraints will lead to what we call a "system failure", which is an event that will render a large cost to the society.

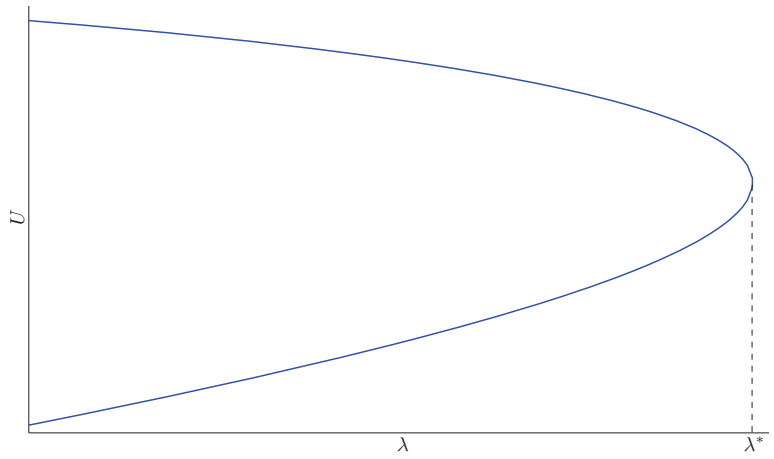

Figure 2.1: A nose curve.

Small signal stability

The system (2.1) is in general of high dimension which makes it hard to analyze its dynamic stability properties. Therefore, many approximate definitions of system stability are given [22]. One approach is to only consider the systems response to small disturbances.

When the algebraic constraints G (in (2.1b)) have an invertible Jacobian G_y along the system trajectories of interest, the algebraic variables can be eliminated

(Implicit Function Theorem [23]) and we get:

$$\dot{z} = F(z, H(z), \Gamma) = \phi(z, \Gamma) \tag{2.2}$$

In small signal stability analysis we look at the properties of the system obtained by linearizing (2.2) around the equilibrium point. Let $z = z_0 + \Delta z$, where z_0 corresponds to a equilibrium point so that $\phi(z_0, \Gamma) = 0$. Then a linearized version of (2.2) is given by

$$\Delta\dot{z} = [F_z + F_y(G_y)^{-1}G_z]\Delta z = A\Delta z. \tag{2.3}$$

Lyapunov's first stability method, which is the fundamental analytical basis for power system small-signal stability assessment, says that (2.1) will remain stable after a small perturbation if the eigenvalues of $A = A(\Gamma)$ all have negative real parts [24].

Therefore, when only considering small disturbances and neglecting the cumulative effect of these disturbances, the transfer capacity can be seen as the level where one (or more) of the eigenvalues of the Jacobian A crosses the imaginary axis. A point in parameter space where one (or more) of the eigenvalues of the Jacobian A crosses the imaginary axis is called bifurcation [25], or structural instability. There are two types of generic local bifurcations that occur in power systems [26]:

Saddle-node bifurcation A Saddle-Node Bifurcation (SNB) is a bifurcation in which two equilibria of a dynamical system collide and annihilate each other. At SNB-points one eigenvalue of A is zero.

Hopf bifurcation Hopf bifurcations are characterized by complex eigenvalues of A crossing the imaginary axis as the system parameters change. Under reasonably generic assumptions about the dynamical system, we can expect to see a small-amplitude limit cycle branching from the equilibrium point.

Hopf bifurcations have been proven not to exist for simple AC lossless system models [27]. However, Hopf bifurcations have been observed in more detailed AC system models that consider transfer conductances and exciter dynamics [28].

Related to the saddle-node bifurcations are switching loadability limits that can occur when a system variable reaches its design limit. This may lead to that one of the eigenvalues of A takes a leap across the imaginary axis. More detail on this phenomenon is given in Section 3.1.

Above it was mentioned that small-signal stability analysis is only valid for small perturbations of system parameters when neglecting the cumulative effects of the perturbations. More formally, to use bifurcation boundaries as stability limits it has to be assumed that the system dynamics acts much faster to dampen oscillations than the parameters change. This assumption was first introduced in [29], as:

Assumption 1. (2.1) varies quasi-statically.

That is, it is assumed that $\Gamma(t)$ varies slowly enough that system (2.1) is well approximated by keeping Γ constant while the dynamics of the system act.

2.2 Steady-state voltage stability

For normal operating conditions a small increase in consumption at a node of the system will lead to a small decrease of the voltage at that node. This behavior will progress until at a certain consumption level the voltage starts slipping. This phenomenon is often referred to as a *voltage collapse* and sometimes the more graphic term *voltage avalanche* is used [14].

A nose curve is a curve showing the relation between a system variable and a parameter. The name nose curve comes from the fact that the curve takes the shape of a nose as depicted in Figure 2.1, where the relation between a loading parameter λ and the voltage U is plotted.

For each $\lambda < \lambda^*$ the power flow equations have two solutions. For steady-state voltage stability considerations the upper solution corresponds to a stable operating point and the lower to an unstable operating point. At the intersection point λ^* these two solutions meet and the system will become unstable if we try to increase the parameter further [30].

Hence, letting

$$f(x,\Gamma) = \begin{bmatrix} F(x,\Gamma) \\ G(x,\Gamma) \end{bmatrix} \tag{2.4}$$

then the system remains steady-state voltage stable as long as there is a $x = x(\Gamma)$ such that following relation is fulfilled:

$$f(x,\Gamma) = 0, \tag{2.5a}$$
$$g(x,\Gamma) \leq 0. \tag{2.5b}$$

Here, the inequality constraints (2.5b) have been introduced to model limitations in generators. Also, voltage limits and thermal stability constraints can be included in the inequality constraints. This is the basis for the SCOPF formulation discussed below.

In this section we have gone through some of the main mechanisms that limit the capacity to transfer power from one node of the system to another. To fully understand the challenges in Q1 and Q2 we also need to understand how the power flow is controlled. But first we take a look at the general structure of the markets on which electric energy is traded.

2.3 Electricity markets

Electrical power is traded in energy per trading period. Usually, trading is performed hourly as on the European Energy Exchange [31], PJM [32], and in the Nordic system [15]. Also, half-hour periods are used in some systems such as for example in UK [33]. The market for trading electric energy is divided into different parts depending on the time left to the actual period of delivery [34]:

- Day-ahead market: This is in general where most of the electric energy is traded. The day-ahead market normally closes at noon on the day before the trading period during which the actual exchange of energy will take place, thus the name day-ahead market. Hence, energy at this market is traded 12 to 36 hours before it is actually delivered.
- Intra-day trading: Intra-day trading offers a possibility to adjust the traded quantities from the day-ahead market according to updated forecasts. It is possible to continuously trade power on this market from that the day-ahead market has closed and the traded quantities and prices have been published, until some time, for example one hour in the Nordic market, before the start of the actual operating period.
- The regulating power market: On this market, the system operator can trade power in order to keep a balance between production and consumption in the system when necessary. In situations with excess power, the system operator can accept bids corresponding to decreasing the net production in the system (downward balancing). In the opposite situation, the system operator calls bids corresponding to increasing the net production in the system (upward balancing). Bids to this market can be submitted shortly before the start of the operational hour. To the Swedish regulating power market bids can be submitted or changed up till 45 minutes before the start of the operational hour [35]. These bids are then activated during the operation period in order to keep the frequency close to the nominal frequency and to handle problems cased by bottlenecks. Bids are usually activated in order of their cost but to handle bottlenecks the cost order sometimes has to be sidestepped.
- Imbalance settlement: The difference between the actual energy consumption / production and the traded quantity is called an imbalance. At the end of each hour the system operator (SO) checks the imbalance for each actor on the electricity market. If a consumer has consumed more energy than he has bought on the markets he has a negative imbalance that he will have to pay for, if he on the other hand has consumed less power than he has bought he will get payed for his positive imbalance.

A time-line displaying the above mentioned trading possibilities is shown in Figure 2.2. As mentioned above the large quantities are usually traded on the day-ahead market, while the intra-day market can be used to decrease the imbalance

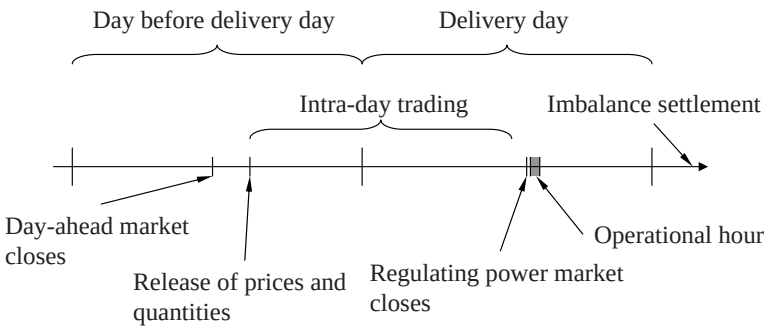

Figure 2.2: Time-line for physical trading of electricity.

between quantities traded on the day-ahead market and the expected production according to updated production forecasts.

It should be noted here that what we denote by regulating market is referred to by different names in different systems; *e.g.* real-time balancing market in PJM [32], real-time energy market in New England [36], frequency control ancillary services (FCAS) market in Australia [37], and regulating market in the Nordic system [15]. A compilation of balance management in Europe can be found in [38].

As mentioned above, bids handed into the regulating market are activated as a part of the frequency control.

2.4 Frequency control

To maintain a balance between generation and production in the system there are three different control systems working together, the primary, secondary and tertiary control [13, 14].

Primary control

In most generators there are large turning masses, which act as storages for energy. When the demand of electric power in a power system increases, energy is taken from this rotating reserve and the frequency in the system drops. As a response to the frequency decrease the power plants with a reserve designated for what is called the primary control will increase their production.

The primary control thus acts as a fast response both to small disturbances such as a change in the loading, and to larger disturbances such as an outage in a power plant.

The power plants that participate in the primary control each have a certain gain, R [MW/Hz], which indicates how the generation of this plant is changed when

the frequency changes.

Example 2.1 If a certain power plant has gain $R = 100$ MW/Hz and the system nominal frequency is $f_0 = 50$ Hz, then at the system frequency $f = 49.9$ Hz the production G in this power plant will have changed $\Delta G = -R \cdot (f - f_0) = -100 \cdot (-0.1) = 10$ MW.

The distribution of the gain between the plants in the system will have a strong influence on the risk of system failure. If, for example, a large part of the gain is located on one side of a bottleneck in the transmission grid, then a failure in a high producing unit on the other side will lead to a highly increased power flow through the bottleneck.

Secondary control

In many systems there is a second, slower acting, automatic control. This control system is called the secondary control and is often administered by having a Automatic Generation Control (AGC) system controlling the production in a subset of the generators [13]. The AGC is often used to divide the system into smaller control areas. The transmission lines connecting the different control areas are called "tie-lines". These tie-lines are operated with agreed upon transfers. The objective of the AGC is, additional to keeping the frequency close to nominal, to maintain the agreed upon transfers on the tie-lines.

Secondary control is mainly used in larger, meshed systems. The Nordic system, for example, does not have any secondary control. In this thesis we will not investigate how to optimize the secondary control. Hence, the main focus will be on bottlenecks either within control areas or in systems that does not have a secondary generation control.

Tertiary control

As mentioned above, in a deregulated market environment the activation of tertiary reserves is equivalent to the activation of regulating bids by the system operator. The tertiary control is thus manually operated in the sense that the system operator receives bids from producers and consumers before the period of operation. These bids are then activated either to relieve the burden on the primary and secondary control, or to keep power flows on acceptable levels.

When a decision is made to activate a regulating bid the system operator contacts the producer (or consumer) responsible for the bid and tells him to change the generation (consumption) in the unit which the bid concerned. Once the call has been made some time has to be allowed before an actual change in power production takes place. Also, physical limitations in the power producing units dictate that no sudden changes can take place. Instead a ramping of the produced power

will occur, which will further delay the execution of the order to activate a bid.

Throughout the work presented in this thesis it is assumed that each regulating bid can be represented by a vector $R_i = (g_i, K_i, \delta_i, \Delta P_i)$, where:

$g_i \in \{1, \ldots, M_g\}$ is the generator to which bid i relates,
$K_i : [0, T] \to \mathbb{R}$ is such that $K_i(t)$ is the total cost induced by activating bid i at time t,
δ_i is the total delay, *i.e.* the time from activation to execution, of bid i, and
$\Delta P_i : [0, \delta_i] \to \mathbb{R}$ is the injected active power ramp function of generator g_i connected to the bid.

Once the call has been made to activate bid i at time η_i the actual corresponding change in production in generator g_i at time $\eta_i + t$, for $t > 0$, will be $\Delta P_i(t \wedge \delta_i)$. We call $\Delta P_i(\delta_i)$ the *total volume* of Bid i. A sketch of a possible shape of ΔP_i is given in Figure 2.3. First, the producer responsible for the bid will have to react and change the setting of power output. Then, δ_i' time units after the activation of the bid, a ramping of the injected power will start. This will result in the bid being executed at δ_i time units after the activation of the bid. It will be assumed that

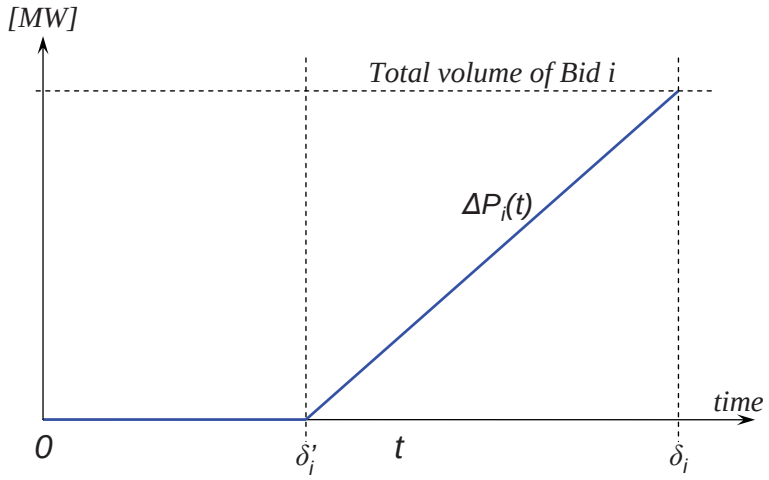

Figure 2.3: A possible shape of ΔP_i.

after activation the bid stays active for the rest of the operation period, so that the activation of a bid is an irreversible process.

Note that with this model it as also assumed that a regulating bid, if activated, is always activated to its full extent. In [39], which is the report of a master thesis project carried out at Vattenfall (energy producer), regulating bids for hydropower

were modeled by at most two blocks. One block from the base case production level to the production level with highest relative production equivalent and one block up to maximal production. This can be modeled as two separate bids by adding the restriction that one bid cannot be activated before the other.

However, without modification the model can not be used for the situation on a non-deregulated market where the system operator owns the power plants and can decide where to change the production and how large the change should be [14].

2.5 Transfer limits

Figure 2.4 depicts an example of what the transfer through one section of the grid, where the flow is not controlled by AGC, may look like. Here, the transfer reaches

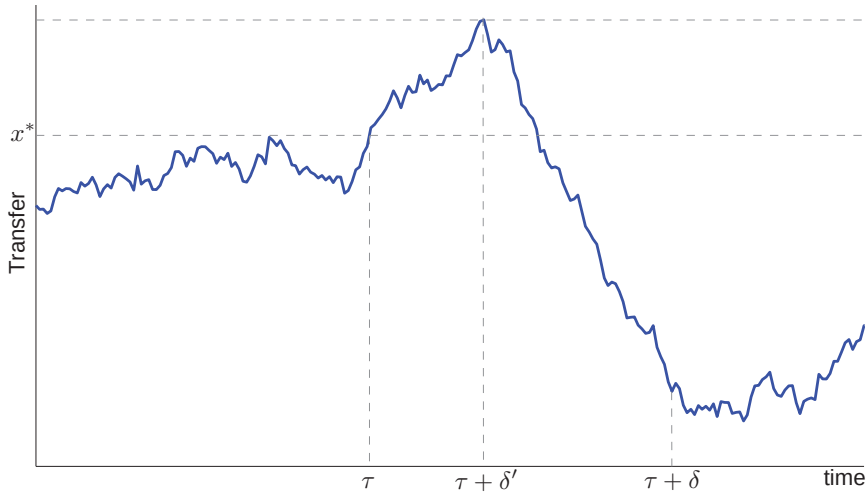

Figure 2.4: The power transfer through a transmission corridor as a function of time. At $t = \tau$, the transfers reach a predefined level x^*, resulting in the activation of a regulating bid. The regulation is then initialized at the delayed time $t = \tau + \delta'$, when a ramp-up of a power plant starts. The order to activate the bid is fully executed at time $\tau + \delta$.

the transfer limit, x^*, at time τ which causes the system operator to activate a regulating bid. If the activated bid was wisely chosen, this will lead to a ramping of the power flow starting at time $\tau + \delta'$ ramping up to its full size at time $\tau + \delta$.

Here, we see that due to lack of flexibility in the tertiary control we not only have to consider the risk of system failure when the transfers are at the level x^*. We also have to consider the risk of system failure following the activation of a

reserve up till that the reserve has increased its production to a level which takes the transfers below x^* again.

With the introduction of more variable energy sources the uncertainties in future net load will increase. Due to lack of flexibility this will thus in turn lead to an increased need for transmission margins and the need for new, more accurate, methods for assessing adequate security margins.

TTC, TRM and NTC

Historically, the decision of adequate transfer limits have built on calculating a physical transfer capacity and subtracting a security margin from this capacity. This approach leads to three different concepts; the Total Transfer Capacity (TTC), the Transmission Reliability Margin (TRM) and the Net Transfer Capacity (NTC). According to the former association Nordel (now part of ENTSO-E) these are defined as follows [12]:

TTC: *TTC is the maximum exchange program between two areas compatible with operational security standards applicable at each system if future network conditions, generation and load patterns were perfectly known in advance.*

TRM: *TRM is a security margin that copes with uncertainties on the computed TTC values arising from:*

a) *Unintended deviations of physical flows during operations due to physical functioning of load-frequency regulation,*

b) *Emergency exchanges between TSOs to cope with unexpected unbalanced situations in real time,*

c) *Inaccuracies, e.g. in data collection and measurements.*

It is also pointed out in [12] that in the Nordic system consideration is, in practice, only taken to a).

NTC: *The Net Transfer Capacity NTC (trading capacity) is defined as:*

$$NTC = TTC - TRM$$

NTC is the maximum exchange program between two areas compatible with security standards applicable in both areas and taking into account the technical uncertainties on future network conditions.

The TTC is thus the transfer capacity when a certain security criterion is applied.

Other definitions of these concepts are given in for example [40, 41].

Criterion based transmission limits

When calculating the TTC a security criterion is often used. The most popular security criterion is the $(N-l)$–criterion [42] which states that the system should be able to withstand the loss of any l system components. To evaluate whether an operating point satisfies the $(N-l)$–criterion, dynamic simulations are performed where the simultaneous failure of l different system components is mimicked [43].

Simulating all possible set of l-component contingencies can be very computationally demanding. However, many contingencies can often be ruled out since others are more severe [42]. The contingencies which have the largest impact on the power system, are called dimensioning faults.

2.6 The Swedish system

We take as an example the Swedish power system. The Swedish system is a part of the Nordic system (see Figure 2.5), which only has DC links tying it together with the main power system of the European continent.

In the one year period prior to May 10, 2009, out of a total electricity production of 137.1 TWh in Sweden, electricity from hydropower accounted for 64.1 TWh (47%), and nuclear power delivered 56.9 TWh (42%). At the same time other thermal plants in Sweden produced 14.2 TWh (10%) while wind power produced 1.8 TWh (1%). Sweden was a net importer of electricity by a margin of 3.3 TWh [44].

A large part of the power production in the Swedish system comes from hydro power plants which are located in the northern parts of the system whereas the main consumption is in the southern part of the country. This means that large amounts of power have to be transferred over long distances. Such situations usually means that the physical constraint limiting transmission is voltage stability.

Frequency control

The Swedish power system is part of the Nordic system and the frequency control reserve is divided between the different countries as shown in Tables 2.1 and 2.2.

Table 2.1: The Nordel agreement on the minimum gain in the frequency-interval 50 ± 0.1Hz. [45]

Area	Gain [MW/Hz]	Reserve [MW]
Sweden	2370	237
Norway	2030	203
Finland	1370	137
Eastern Denmark	230	23
Synchronous System	6000	600

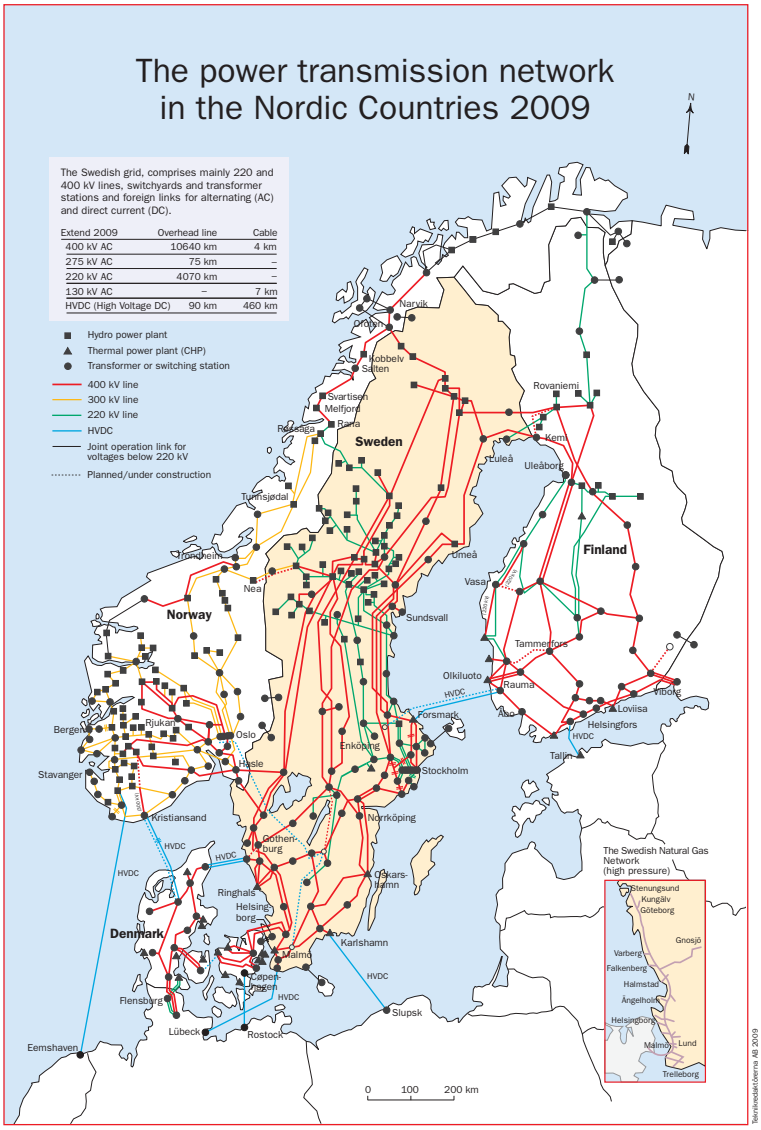

Figure 2.5: The Nordic power system.

The main part of the primary frequency control in the Nordic system is in the hydro power plants which are located in northern Sweden and in Norway. This means that an increase in load or an outage in a power plant in the south of Sweden is balanced in the north.

Table 2.2: The Nordel agreement on the minimum gain in the frequency-interval $(49.5, 49.9)$Hz. [45]

Area	Gain [MW/Hz]	Reserve [MW]
Sweden	805	322
Norway	792.5	317
Finland	570	228
Eastern Denmark	382.5	153
Synchronous System	2550	1020

The Nordic system does not have any secondary frequency control.

The tertiary control reserves are provided through a regulating power market. Bids to this market can be handed in or updated continuously from 14 days up till 45 minutes before the operational hour in question. After this all bids handed in to the market are financially binding [35].

All bids handed in to the regulating market should specify a volume (MW), a price (€/MWh), a total delay δ (min) and the unit which the bid concern [35].

The volume of a bid can only be divided if a special agreement is made between the actor responsible for the bid and Svenska Kraftnät. The agreement of purchase of regulating power ends at the end of each operational hour, unless special agreements have been made [35].

Transfer limits

The system operator of the Swedish power system, Svenska Kraftnät, monitors the transmission through three chosen transmission corridors (bottlenecks) as depicted in Figure 2.6. The TTC through each transmission corridor is set using the $(N-1)$–criterion [47]. For each corridor, a number of nodes where the load is assumed to increase are chosen. Each of these nodes are then given a load increase factor. By stepwise increasing each load according to its load increase factor and simulating the dimensioning faults the TTC through the specific corridor is calculated. Then a reserve margin (TRM) is subtracted from the TTC to get the NTC [47].

To make sure that the transfers do not violate the TTC, Svenska Kraftnät activates bids on the regulating market when the flows approach the NTC. In the Nordic system, which can be considered to be a non-meshed net, choosing an appropriate regulating bid is simpler. If, for example, the transfers through the southern bottleneck approaches the NTC, Svenska Kraftnät will activate the cheapest bid south of the bottleneck. This will lead to a decrease in production north of the bottleneck and thus reduce the southward flow through several bottlenecks including the southern one. Another option is to simultaneously activate a downward-regulating bid in Elområde Stockholm (SE3) (see Figure 2.6). In this way the flow through

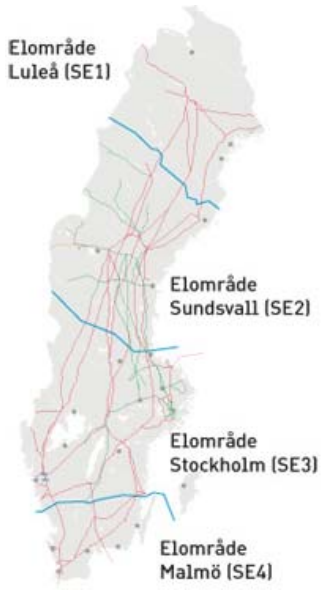

Figure 2.6: The three bottlenecks dividing the Swedish system into four areas [46].

the southern bottleneck can be controlled without interfering too much with the other flows or the frequency.

2.7 State-of-the art in power system operation

As described above, power system operation is closely related to congestion management, *i.e.* management of system bottlenecks. In the previous section we discussed how this can be performed in the Swedish system.

If the areas of the power system are aligned in a straight line it is easy to realize how a rescheduling of the production will influence the flows through the critical transmission corridors. In large meshed networks it may be hard to determine how flows will change when the generation in one plant is increased.

One option here is to approximate the change in flows by the Generator Shift Factors (GSFs). The GSFs approximate the change in flow on a particular transmission corridor that results from increasing generation at a node [48]. Using the GSFs it is thus possible to estimate which regulating bid is most appropriate to activate.

Another way of maintaining secure operation is by rescheduling production according to the solution to a Security-Constrained Optimal Power Flow (SCOPF).

SCOPF

The state-of-the-art when including security constraints in power system planning is Security-Constrained Optimal Power Flow (SCOPF) [49]. In SCOPF some security criterion, for example the $(N-l)$–criterion, is selected. The optimal distribution of generation is then found by solving a large optimization problem with fulfillment of the security criterion as constraints. The SCOPF problem can be formulated as:

$$\min_{x_0,\ldots,x_{n_c},u} \quad C(x_0,u) \tag{2.6a}$$

$$\text{s.t.} \quad f_j(x_j,u,\lambda)=0 \quad j=0,\ldots,n_c \tag{2.6b}$$

$$g_j(x_j,u,\lambda)\leq 0 \quad j=0,\ldots,n_c \tag{2.6c}$$

where $C:\mathbb{R}^{n_{x,0}+n_u}\to\mathbb{R}$ is the objective function, in most cases representing the total production cost, $f_0:\mathbb{R}^{n_{x,0}+n_u+n_\lambda}\to\mathbb{R}^{n_{e,0}}$ and $g_0:\mathbb{R}^{n_{x,0}+n_u+n_\lambda}\to\mathbb{R}^{n_{i,0}}$ are the equality and inequality constraints for the base case, $f_j:\mathbb{R}^{n_{x,j}+n_u+n_\lambda}\to\mathbb{R}^{n_{e,j}}$ and $g_j:\mathbb{R}^{n_{x,j}+n_u+n_\lambda}\to\mathbb{R}^{n_{i,j}}$ are the equality and inequality constraints for post-contingency state j, for $j=1,\ldots,n_c$, with n_c the number of contingencies considered, $x_j\in\mathbb{R}^{n_{x,j}}$ is a vector of state variables post contingency j, $u\in\mathbb{R}^{n_u}$ is a vector of control variables, *e.g.* the output of certain generators, and $\lambda\in\mathbb{R}^{n_\lambda}$ is a vector of parameters, for example the system loading.

In the SCOPF problem it is also possible to allow post-contingency corrective rescheduling as described in [50].

In [13] the following suggestion of how SCOPF can be used in power system operation is given:

> Using either the current state of the power system or a short-term load forecast, the OPF can be set up to provide a "preventative dispatch" if security constraints are incorporated.

Here, incorporating security constraints in the optimal power flow (OPF) means that we get a SCOPF. By choosing the time frame of the short-term load forecasting to correspond with the reaction times of the tertiary control we can thus account for the lack of flexibility in the generation control.

From the SCOPF formulation we can get a more stringent definition of the TTC. The parameter space equivalent of TTC is the boundary of the domain given by the constraints (2.6b) and (2.6c).

When choosing the list of contingencies one should consider the following argument from [51]:

> It is almost a folk theorem that major failures in complex engineering systems, such as power grids, result from the simultaneous occurrence of several rare events, or unusual operating conditions, the combination

of which would not have been identified as a plausible subject for study a priori.

Hence, a large number of contingencies have to be considered which will make the number of contingencies to be analyzed online when solving (2.6) huge. To be able to handle this contingency filtering techniques such as the ones proposed in [49, 52] can be used.

If using SCOPF to set rules for operation it is possible to, for a large number of different system parameter settings, find the cost-optimal way of running the system. However, when using SCOPF to decide a strategy for the activation of regulating bids the method has some shortcomings.

i) It is hard to consider the structure of the market at which regulating power is traded. This structure will make it impossible to exactly follow the path of the optimal $u(t)$ when random fluctuations act on the system parameters $\lambda(t)$.

ii) Also, we only use a forecast of the future demand which will be less accurate with the inclusion of more variable generating sources.

iii) By using a security criteria no efficient balancing of risk of failure versus operation cost is performed. The constraint imposed by any contingency included in the analysis is never allowed to be violated.

Probabilistic power flow

In a regular power flow calculation, system parameters, such as loads at load buses and generator set-points, are given by a vector $\Gamma \in \mathbb{R}^{n_u+n_\lambda}$, and the corresponding values of system variables $x \in \mathbb{R}^{n_x}$ are given by solving a system of n_x equations, $f(x, \Gamma) = 0$. In probabilistic power flow a subset of the parameters is assumed to be stochastic and have a known multivariate probability distribution. Then a series expansion of the power flow equations is used to approximate the distribution of system variables.

One interesting application here is to try to approximate the probability distribution of power flows through transmission corridors. We start with a base case operating point. Then the Power Transfer Distribution Factors (PTDFs) [48], which give the linearized relation between injected power in one node and power flow through transmission corridors, can be obtained through the power flow equations. If we denote by A the matrix of PTDFs of interest, this can be written

$$\Delta P_{Tr} = A\Delta\Gamma, \tag{2.7}$$

where ΔP_{Tr} is the change in power flows, corresponding to the change in parameters $\Delta\Gamma$. Now, the probability that the power flow through transmission corridor j exceed a certain threshold b_j can be written $\mathrm{P}[P^{(j)}_{Tr,0} + \Delta P^{(j)}_{Tr} > b_j] = \mathrm{P}[a_j\Delta\Gamma >$

$b_j - P^{(j)}_{Tr,0}]$, where a_j is the j^{th} row of A and $P_{Tr,0}$ are the base case flows. By using the cumulants [53] to represent $a_j\Delta\Gamma$, as in [54], the sought probability can be computed through the Cornish-Fisher expansion [55] (see [48] and references therein for details).

P-OPF

In Probabilistic Optimal Power Flow (P-OPF) some parameters are considered to be random and the distribution of system variables corresponding to the optimal generation dispatch is sought. Assume that $(x_0^*(\lambda), u^*(\lambda))$ is the optimal solution to (2.6) corresponding to λ. The objective of P-OPF is to find the probability distributions of $x_0^*(\lambda)$ and $u^*(\lambda)$ given the probability distribution of λ.

The solution to the P-OPF will, thus, provide means of finding confidence bounds for the system variables over long time periods. This makes P-OPF suitable for long-term planning.

P-OPF was introduced in the beginning of the 1980's [56]. Since then P-OPF has attracted much interest from researchers [57–61].

S-OPF

At almost the same time as P-OPF was introduced, so was Stochastic Optimal Power Flow (S-OPF) [62]. S-OPF was introduced to be able to account for uncertainties in system parameters in the OPF problem. S-OPF is thus, as opposed to P-OPF, a stochastic programming problem. Examples of papers dealing with S-OPF include [63–65].

In [48, 62] the uncertainties enter the constraints only and we get the situation described below.

Assume that $\Gamma_0 = (u_0, \lambda_0) \in \mathbb{R}^{n_u+n_\lambda}$ is a base case (forecasted) parameter vector and that the actual parameter vector is given by $\Gamma = \Gamma_0 + \Delta\Gamma$, where $\Delta\Gamma = (\Delta u, \Delta\lambda) \in \mathbb{R}^{n_u+n_\lambda}$ is such that $\Delta u \in \mathbb{R}^{n_u}$ is the change of controllable system parameters, such as set-points of generators, and $\Delta\lambda \in \mathbb{R}^{n_\lambda}$ is the difference between the base case and the actual case (*i.e.* the forecast error). When trying to optimize the choice of Δu to minimize production cost while maintaining a certain degree of security for each congested transmission corridor we get a S-OPF problem. The S-OPF problem can thus be defined as:

$$\min_{\Delta u \in U - u_0} \quad C_G(u_0 + \Delta u) \tag{2.8a}$$

$$\text{s.t.} \quad \mathrm{P}[P^{(j)}_{Tr,0} + a_j\Delta\Gamma > b_j] \leq \alpha_j, \quad j = 0, \ldots, n_{TC} \tag{2.8b}$$

where $C_G : U \to \mathbb{R}$ is the net cost (¤/h) of production dispatch, $P^{(j)}_{Tr,0}$ is the transfers corresponding to the base case, the α_j are small numbers, the b_j are calculated transfer capacities and n_{TC} is the number of congested transmission corridors.

In [65] the random parameters also enter the objective function.

By solving a S-OPF problem we can thus obtain the optimal dispatch needed to keep transfers on acceptable levels, with a certain probability for each corridor, for a future system state.

This is an improvement over the SCOPF method where no regard is taken to uncertainties in future injected power from load and variable generating sources. Hence, shortcoming ii) of the SCOPF is taken care of with the S-OPF. However, the task of deciding $b = (b_1 \cdots b_{n_{TC}})$ and choosing the α_j arise instead.

One problem with S-OPF is that the problem formulation does not give the probability that the transfers through all corridors stay below their respective transfer capacity. All we know is that this probability does not exceed $1 - \sum_{j=1}^{n_{TC}} \alpha_j$. What we would like is to replace the constraint (2.8b) with

$$\mathrm{P}[P_{Tr} > b] \leq \alpha, \tag{2.8b'}$$

for some $\alpha > 0$. Unfortunately, finding an analytical solution to this problem seems to be out of reach.

2.8 Power system operation approach in this thesis

The power system operation strategy presented in this thesis is not based on a security criterion. Instead it is suggested that contingencies should be evaluated in a Monte Carlo simulation. This Monte Carlo simulation will, by assigning a cost to each type of system failure, estimate the expected cost of operation from failures as a function of the setting of the n_u controllable system parameters and a set of k observable system variables. The observable system variables will be referred to as the *observables*. This Monte Carlo simulation should be performed as a pre-study and the resulting cost function can be seen as specific to the system.

Close to the period of operation, a stochastic model of the observables should be estimated and stochastic control methods are to be applied in order to find the strategy for activation of regulating bids that minimize the expected operation cost for the operation period $[0, T]$. Here, operation cost will include both net cost from rescheduling production and expected cost to the society from system failures.

A schematic sketch of the proposed method is given in Figure 2.7. First a list of contingencies to be evaluated is chosen and a load pattern type is decided. The load pattern type should reflect aspects such as time of day, day of week and seasonality. Then the values of the controllable system parameters u and the observable system parameters θ are chosen. Given (u, θ) the full parameter vector λ is randomized. To obtain the expected cost from system failures the result of every contingency in the contingency list is evaluated. Then, by assigning a specific cost to each type of system failure and multiplying the cost by the probability of the contingency leading to the system failure, the expected cost of failures is obtained.

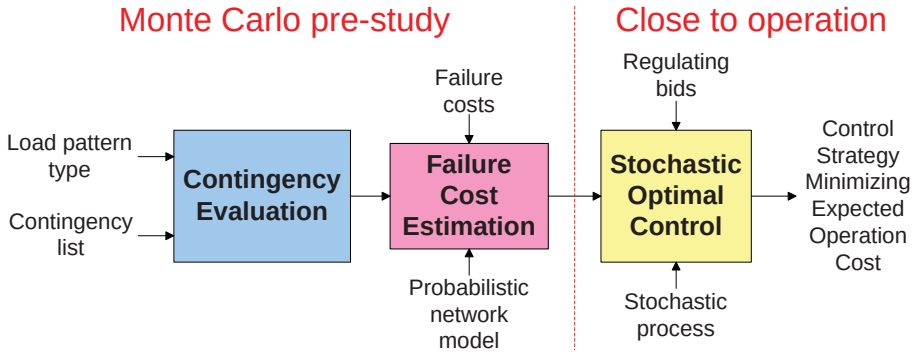

Figure 2.7: Schematic sketch of the approach outlined in this thesis.

After that no more bids can be handed in to the regulating market we chose a stochastic process to model the observables and optimize the activation of regulating bids during the operation period. It is preferable that this is done close to the actual period of operation so that the best possible stochastic model can be used.

With the proposed method it is possible to obtain an adequate balance between transmission and security. Also, the tertiary control can be modeled in an accurate way, including reaction times and ramp rates for all participating power plants. The trade-off is that due to the necessity of numerical tractability the number of observables is limited.

Relation to existing methods

To end this background chapter we summarize the stochastic control approach described in this thesis, SCOPF and S-OPF.

SCOPF

Aim Given a parameter vector, find a generation dispatch that minimizes the expected cost of production such that the corresponding operating point satisfy a given security criterion.

Physical constraints In general only load flow feasibility and voltage limits are included, but crude estimates of dynamic stability can be included as limits on line transfers [49].

Contingencies The contingencies considered are given by a contingency list. The solution has to be able to manage all contingencies in the list.

Operation boundary Incorporated contingencies together with physical constraints define a strict operation boundary in parameter space.

Time-frame One single point.

Load model Deterministic.

Comment The deterministic load model and the time frame considered makes SCOPF more useful for controlling AGC, since AGC provides a continuous and fast control of the power generation as opposed to the more impulse like control provided by the tertiary control. SCOPF gives a clear definition of TTC, but fails to include a risk based TRM.

S-OPF

Aim Given the probability distribution of the parameter vector, find a generation dispatch that minimize expected cost of production such that a given set of system variables does not violate given constraints with a certain probability for each constraint.

Physical constraints In general only limits on line flows and voltage limits are included, but crude estimates of dynamic stability can be included as limits on line transfers [49].

Contingencies Can use a full probabilistic network model but this will make solution very difficult [48]. More reasonable is to calculate a TTC and operate the system so that the TTC is not violated with a certain probability.

Operation boundary Each of the physical constraints included have to be satisfied with a certain given probability. Hence, no strict operation boundary exists.

Time-frame One single point.

Load model Multi-dimensional random variable representing the nodal loading.

Comment Makes up for the lack of handling randomness in the SCOPF. Fairly easy to implement. Only restricts the probability of violating the constraints one at a time (compare (2.8b) to (2.8b')). Can be used to calculate a risk based NTC.

New stochastic control approach

Aim Calculate a strategy for activating regulating bids that minimize the expected cost of operation. Here, operation costs are production costs plus costs from failures. The strategy should be based on the values of a set of observable system variables.

Physical constraints Monte Carlo simulation is used to estimate the cost of failure given a set of transfers. This means that any physical constraints can

be incorporated. However, we will focus on situations when the load satisfies Assumption 1 of Section 2.1, and only saddle-node bifurcations exists.

Contingencies Contingencies will be included in the Monte Carlo simulation. As with SCOPF, a list of contingencies will be analyzed. However, an economical balancing of security versus transfer will be made so that the operating point does not have to survive all analyzed contingencies. This means that more contingencies can be added to the list without interfering to much with the transfer limit.

Operation boundary The economical balancing renders that the contingencies analyzed will not define a strict operation boundary. However, the non-contingency state load flow feasibility will be used to define a strict operation boundary for the observables.

Time-frame Considers entire trading period.

Load model Multi-dimensional Markov process models the observables.

Comment With this method we more accurately model the controllability limitations of the tertiary control, including the fact that any decision made now will influence the future. The power system is reduced to a cost function in the controllable system parameters and the observable system variables. This means that we do not have to assume that the entire system state is known to the operator. To obtain the cost function, an extensive pre-study (the Monte Carlo simulation to estimate the expected cost from failure) has to be performed. The method cannot, without modification, be applied to optimize the secondary control. It is currently unknown how well the method scales to systems with a large number of observables.

Chapter 3

Estimating the risk of system failure

This chapter deals with the evaluation of the risk induced by keeping a certain transfer level. The main challenge we face here is that, due to lack of flexibility in the generation control, we have to estimate the risk of system failure within a short time following any contingency. Short introductions to Articles I–V are given in this chapter.

In the discussion of state-of-the-art methods for power system operation in Section 2.7 two interesting methods were investigated, Security Constrained Optimal Power Flow (SCOPF) and Stochastic Optimal Power Flow (S-OPF). It was also pointed out that (as proposed in [13]) to use SCOPF for operational purpose a forecast of the system parameters could be used as input to the SCOPF when optimizing the generation dispatch. This approach fails to take into account the uncertainty in future operating states due to uncertainty in demand and generation from variable generating sources, such as wind power. A better method that considers also the uncertainty in future parameter values is given by the S-OPF.

What gives the S-OPF the ability to handle uncertainties is the probabilistic power flow formulation which approximates probability distributions for flows by linearizing the relation between injected power and transfer through transmission corridors. This gives the constraints (2.8b) to the S-OPF problem.

As mentioned in the previous chapter there are several different constraints that may define the physical transfer capacity. In this chapter we will focus on steady-state voltage stability [17].

In articles III and V (and [7]) we try to find a way of estimating the risk of voltage instability within a certain time-frame. This can be seen as a more accurate voltage stability equivalent of the power flow constraint (2.8b). The idea to our problem formulation came from the pioneering work in [16], which unfortunately suffers from some inconsistencies (see [7] for more details). In order to estimate the

risk of voltage instability we need to develop a stochastic model for the consumption, which is done in Article I.

In our method, decisions will be based on the values of a number of observable system variables, which will in general represent the flows through certain "critical" transmission corridors. A method for generating parameter values that give certain transfers were developed in Article II.

In this chapter brief introductions to the above mentioned articles will be given along with an introduction to voltage stability in Section 3.1 and a discussion on how the probability of system failure can be calculated in Section 3.2. In Section 3.4 we summarize how the operation cost function and the operation boundary are built.

3.1 Loadability limits

Steady-state (or long-term) voltage stability is closely connected to power system loadability in the sense that the steady-state voltage stability limits equal the power system loadability limits in parameter space.

The following equality-inequality constraint representation of the steady-state of a power system was introduced in [17]:

$$\psi(x, u, \lambda) = 0, \tag{3.1a}$$

$$f^{a,i}(x) \cdot f^{b,i}(x) = 0, \quad i = 1, \ldots, n_s, \tag{3.1b}$$

$$f^{a,i}(x) \geq 0, \quad i = 1, \ldots, n_s, \tag{3.1c}$$

$$f^{b,i}(x) \geq 0, \quad i = 1, \ldots, n_s. \tag{3.1d}$$

Here, ψ is a smooth function representing the power system. The $f^{a,i}$ and the $f^{b,i}$ are called switching functions and are also smooth. The switching constraints are introduced in order to take account of controller limits imposing constraints on the power system control parameters. One such limiting constraint is due to the overexcitation limiters in the generators of the system. In unconstrained operation the generator excitation EMF E_f is in equilibrium given by

$$0 = -E_f^i + K_A^i \left(V_{ref} - V^i\right) = f^{a,i}(x). \tag{3.2}$$

However, limits on the generator excitation EMF dictate that

$$-E_f + E_f^{lim} = f^{b,i}(x) \geq 0. \tag{3.3}$$

A point in parameter space where, for some $i \in \{1, \ldots, n_s\}$, $f^{a,i}(x) = f^{b,i}(x) = 0$, is referred to as a breaking point [66] due to the shape that the PV-curve takes at such points, or a constraint switching point [67]. At such points the limit of the control variable, in this case E_f, is reached and the set of active constraints change.

From an initial operating point (x_p, u_p, λ_p) satisfying the feasibility constraints (3.1a)-(3.1d) the loadability limit in the direction of stress $d \in \mathbb{R}^{n_\lambda}$ is the solution

to the equality-inequality constrained optimization problem

$$\max_{x\in\mathbb{R}^n, s\in\mathbb{R}_+} \{s : (3.1a) - (3.1d) \text{ holds with } u = u_p \text{ and } \lambda = \lambda_p + sd\}. \tag{3.4}$$

Solution methods to this optimization problem have been intensively investigated and include continuation methods [68–70]. In the continuation method first the parameters are increased along the direction d as $\lambda = \lambda_p + sd$. Then a critical state, such as the voltage at a critical bus, is detected and this state is chosen as the continuation parameter. We then continue to seek for the largest possible s by changing the continuation parameter. This will avoid problems caused by the fact that the jacobian matrix of the power flow equations at the loadability limit may be a singular point of the system.

There are two possible scenarios. Either the maximum is obtained at a point without a breaking point, as in Figure 3.1. This is called a Saddle-Node Bifurcation (SNB). At such points the system Jacobian is singular. The other possible scenario

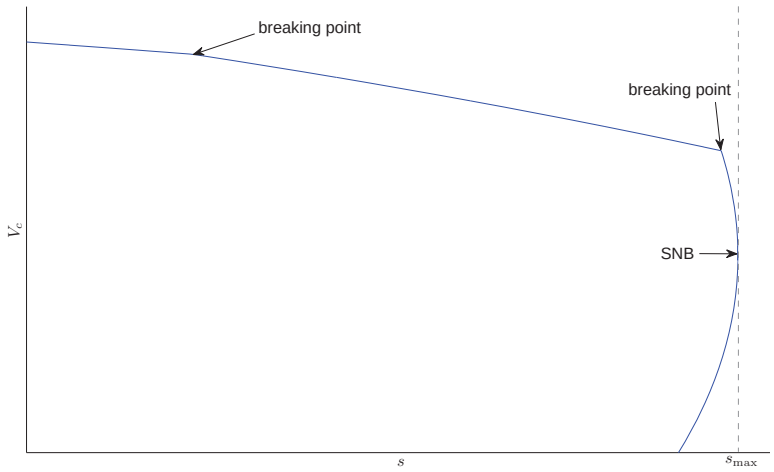

Figure 3.1: A nose-curve with a SNB point.

is that the maximum is reached at a point where we have a breaking point. This is referred to as a Switching Loadability Limit (SLL). An example of a SLL is given in Figure 3.2.

3.2 The risk of system failure

The risk of system failure is related to the distribution of the generation, the loading level and the probability of having different contingencies. An estimate of the risk

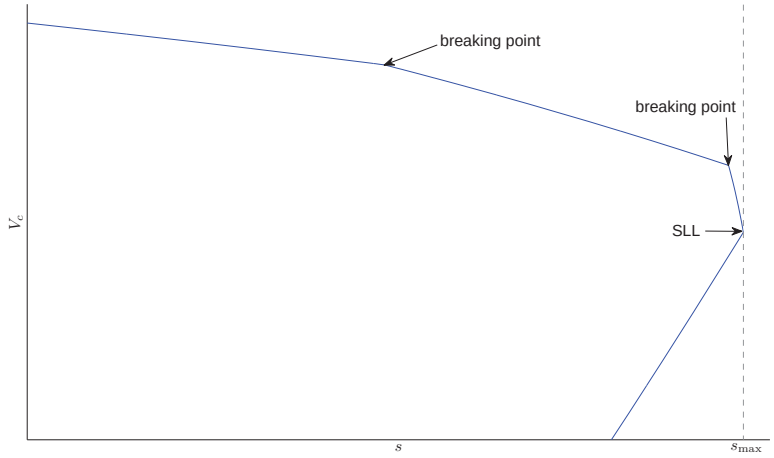

Figure 3.2: A nose-curve with a SLL point.

of system failure, per time unit, is given by

$$r_{\text{fail}}(t, u, \lambda) = \sum_{j=1}^{n_c} r_j p_{\text{fail},j}(t, u, \lambda), \tag{3.5}$$

where n_c is the number of contingencies to be analyzed, r_j is the failure rate connected to contingency j and $p_{\text{fail},j}(t, u, \lambda)$ is the probability of system failure in case of contingency j at time t when the controllable parameters are u and the uncertain parameters are λ. What contingencies that should be analyzed is something that has to be decided individually for each system and is often chosen using a criterion such as the $(N-l)$–criterion or in a more heuristic way based on knowledge of the system. The failure rate, r_j, connected to each contingency is something specific to system components. What remains is to decide $p_{\text{fail},j}(t, u, \lambda)$.

For any type of physical limitations and any contingency to be analyzed, the system failures can be split into two groups depending on when the failure occurs.

i) We get an immediate system failure at the time of the contingency.

ii) No immediate system failure occurs, but the stability margin is so deteriorated by the contingency that a system failure occurs before any emergency response to the contingency have time to take place.

In point i) when we say immediate instability we mean that the operating point in the post-contingency state is not in the domain of attraction of any stable operating point, or the thermal stability limits, for one or more power-lines, are violated which lead to cascading failure [71].

An important factor in ii) is the emergency response time δ_{ER} (unfortunately, denoted by T in the articles of this section) after which we assume that the risk of system failure is reduced enough that the chance of having a future system failure can be neglected.

Let $(\lambda_t)_{t\geq 0}$ be a path in uncertain parameter space representing, for example, the loads at all nodes as a function of time. Let us consider the non-contingency case, where all system components are fully functional. The surface of loadability limits, $\Sigma_0 = \Sigma_0(u) \subset \mathbb{R}^{n_\lambda}$, will then be the outer boundary of a domain $D_0 = D_0(u) \subset \mathbb{R}^{n_\lambda}$ in injected-power space in which each point corresponds to a feasible operating point.

Now let $j \in \{1, \ldots, n_c\}$ represent a specific contingency that occurs at time $t = t_c$. For every j there is a subset $D_0^j \subset D_0$ such that the system will remain stable in case contingency j occurs if and only if $\lambda_{t_c} \in D_0^j$. Hence, i) corresponds to the case when $\lambda_{t_c} \notin D_0^j$.

After a contingency the system will in general be weakened and have a new loadability domain D_j, which is in some sense smaller than D_0. We denote by Σ_j, the boundary to D_j. Hence, Σ_j is the loadability surface after contingency j. Part ii) above corresponds to having a λ_t outside of D_j, within the emergency response time, *i.e.* in the time interval $[t_c, t_c + \delta_{\mathrm{ER}}]$.

In Figure 3.3 the two different situations are depicted for a two-parameter system. When contingency c_1 occurs, then either the parameters are such that im-

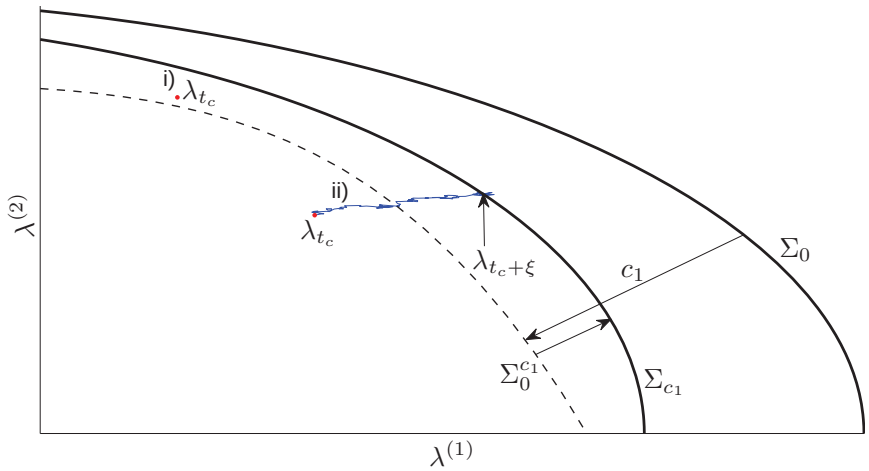

Figure 3.3: Analyzing a contingency. In the figure the dashed line represents the boundary $\Sigma_0^{c_1}$ to the domain $D_0^{c_1}$.

mediate instability occurs. This is the case labeled i). If the parameter values are such that the system remains stable after the contingency, then the parameters may still drift towards the set of unstable points. In the figure, the case labeled ii) rep-

resents a case where the system becomes unstable ξ time units after the contingency.

Remark The two different types of system failures listed above are not the only types of possible system failures. For example, the system can lose dynamic voltage stability due to the small random perturbations on the system driven by changing loads as investigated in, for example [72, 73]. Although inclusion of such events into the failure rate is an interesting topic it has been left as a future work.

3.3 Articles

Article I

In Article I a stochastic model of the power demand in the different areas of a multi-area power system is developed. The demand is modeled by a multi-dimensional Ornstein-Uhlenbeck process. It is shown how the parameters in the Ornstein-Uhlenbeck process can be estimated from hourly measurements of the energy consumption in the different areas. In a case study data from the Swedish, the Norwegian and the Finnish system is used to estimate the parameters of a three-area model.

Article II

One of the difficulties encountered when estimating the risk of voltage instability given a specific set of transfers is the distribution of the load amongst the nodes of the system. Given transfers P_{Tr} we want to be able to generate samples of λ_{t_c}. In Article II we propose a sampling technique that can solve this task. The sampling technique is based on Markov Chain Monte Carlo (MCMC).

Remark Although the presentation in this article is focused on the case when the transfers through k transmission corridors are observed, the method is applicable to any type of observables which depend smoothly on the system parameters.

Article III

If the initial uncertain parameter vector λ_{t_c} is inside D_0^j, we need to estimate the probability that we leave D_j in the coming δ_{ER} time units. This probability can be expressed as

$$F_\xi(\delta_{\mathrm{ER}}; t_c, u, y) = \mathrm{P}\left[\{\inf\{t > t_c : \lambda_t \notin D_j(u)\} | \lambda_{t_c} = y\} \leq t_c + \delta_{\mathrm{ER}}\right]. \qquad (3.6)$$

In Article III we show how $F_\xi(\delta_{\mathrm{ER}}; t_c, u, y)$ can be estimated for a class of stochastic processes. Here, a hyperplane approximation of Σ_j is used to estimate $F_\xi(\delta_{\mathrm{ER}}; t_c, u, y)$. This estimate is then improved using a second order approximation of Σ_j.

In this article we also consider estimation of the distance from λ_{t_c} to the point of collapse, which is the point of Σ_j where λ_t leave the domain D_j.

Article III is a further development of [7] which is why [7] was not included in the thesis.

Article IV

The method outlined in Article III is dependent on local approximations of the loadability surface Σ_j. At most points Σ_j is smooth. However, there are certain parts of codimension one in Σ_j where the surface is non-smooth. In Article IV we compute the distance from a point of Σ_j to the closest non-smooth part. This distance is connected to the validity of local approximations of Σ_j.

Article V

In Article V we focus on the same problem as in Article III. However, the proposed solution is instead by Monte Carlo simulation and the efficiency of using importance sampling on this problem is investigated.

The importance sampling change of measure also provides a severity index for the different contingencies.

Remark Although the focus in the articles of this section is on loadability limits the theory presented can easily be generalized to consider also the Hopf bifurcation surface. The expression for the normal vector to a Hopf bifurcation surface is given in [74]. From this the second fundamental form can be obtained by using equations (5) and (11) from [75].

3.4 The operation cost and the operation boundary

In this chapter we have investigated how to estimate the risk of system failure. This gives us the rate, $r_{\text{fail}} : [0,T] \times \mathbb{R}^{n_u} \times \mathbb{R}^{n_\lambda} \to \mathbb{R}_+$, at which system failures occur. This failure rate can be divided into rates for the different types of failures i) and ii).

We can estimate the cost rate from failures as

$$C_f^{u.p.}(t,u,\lambda) = \sum_{j=1}^{n_c} r_j \left(\mathbb{1}_{\lambda \notin D_0^j} C_f^{\text{i)}}(t,u,\lambda) + \mathbb{1}_{\lambda \in D_0^j} C_{f,2}(t,u,\lambda) \right), \tag{3.7}$$

where $C_f^{\text{i)}} : [0,T] \times \mathbb{R}^{n_u} \times \mathbb{R}^{n_\lambda} \to \mathbb{R}_+$ is the expected cost to society when having a system failure of type i) and

$$C_{f,2}(t,u,\lambda) = C_f^{\text{ii)}} F_\xi(\delta_{\text{ER}};t,u,\lambda) + C_{\text{ER}}(t,u,\lambda)(1 - F_\xi(\delta_{\text{ER}};t,u,\lambda)) \tag{3.8}$$

where $C_f^{\text{ii)}} > 0$ is the expected cost to society when having a system failure of type ii) and $C_{\text{ER}} : [0,T] \times \mathbb{R}^{n_u} \times \mathbb{R}^{n_\lambda} \to \mathbb{R}_+$ is the expected cost of the emergency

response action and for the remainder of the period.

A failure of type i) may lead to events ranging from system separation to a total system blackout. In case of a failure of type ii) the system may be saved by disconnecting some of the load. The cost of disconnecting load will in general be much smaller than the cost of a total system blackout. For more information on interruption costs and customer damage functions see [76] and references therein. An example of a previous work which includes cost of emergency response actions and load disconnection is [77] where a SCOPF problem including costs for security measures in case of contingencies is solved.

In the setting above $C_f^{u.p.}$ is a function of the uncertain parameter vector λ. However, as mentioned in the previous chapter, decisions will be based on the values of a vector $\theta \in \mathbb{R}^k$ of observable system variables, which can be calculated from the controllable parameters u and the uncertain parameters λ, *i.e.* $\theta = h(u, \lambda)$ for some $h : \mathbb{R}^{n_u+n_\lambda} \to \mathbb{R}^k$. Hence, to evaluate the operation cost we need to go from the observables to the uncertain parameters.

One problem that arises here is that the system state is not completely determined by the observables θ (in general $n_\lambda \gg k$). This means that $h(u, \cdot)$ is not invertible so some extra information has to be used when going from (u, θ) to λ. In Article II this was solved by assuming a known probability distribution of the nodal loading. With this method a grid of points for θ can be examined. Another possibility is to let the uncertain parameter vector be a function of k new parameters $\lambda = \lambda(\zeta_1, \ldots, \zeta_k)$ such that a relation can be found between $\zeta = (\zeta_1, \ldots, \zeta_k)$ and the observables. Assume for example that the we have a two area system where the observables are the transfer between the two areas, Area A and Area B, and the system frequency. Let $\lambda = (\lambda^A, \lambda^B)$, where λ^i is a vector of the nodal loadings in Area i. If we assume that $\lambda^i = \lambda_0^i + \zeta_i \lambda_d^i$ then there is a one-to-one relation between ζ and θ.

The resulting function which will be denoted $C_f : [0, T] \times \mathbb{R}^k \times \mathbb{R}^{n_u} \to \mathbb{R}_+$ is allowed to be a function of time, the observables θ, and the controllable system parameters.

To be able to decide whether to activate a regulating bid or not, we need to add the cost of the primary control to the expected cost from failures. After adding the (expected) cost of the primary control, per time unit, to C_f we get the *cost rate function* $f : [0, T] \times \mathbb{R}^k \times \mathbb{R}^{n_u} \to \mathbb{R}$.

Remark As discussed in Section 6.2 the above outlined approach has some serious drawbacks for large k. The solution to this problem, which is outlined in Section 6.2, is to use regression to approximate f as the sum of a sequence of representative functions.

Remark In this section f is allowed to be a function of time. However, assuming that $(\lambda_t)_{t\geq 0}$ is a stationary Markov process, for example a scaled Brownian motion

with drift, it would be possible to drop the time dependence. Instead, one can estimate a few different $f : \mathbb{R}^k \times \mathbb{R}^{n_u} \to \mathbb{R}$ depending on season, day of week and time of day.

The operation boundary

We denote by $\mathcal{S} \subset \mathbb{R}^{n_u+k}$ the feasible operation domain of the non-contingency system ($\mathcal{S} \subset [0,T] \times \mathbb{R}^{n_u+k}$ if the operation domain depends explicitly on time). We assume that reaching the boundary $\partial\mathcal{S}$ to the operation domain is something that should at all times be avoided since this renders the system operator a large expected cost. For example, reaching the saddle-node bifurcation boundary is something that may lead to voltage collapse.

When building the operation boundary the same problem as before arises. One possible approach here is to define the inverse, h_u^{-1}, of $h(u,\cdot)$ as a selection of $h_I(u,\theta) \in \operatorname*{Argmax}_{y\in\mathbb{R}^{n_\lambda}}\{f_\lambda(y) : \theta = h(u,y)\}$, where $f_\lambda : \mathbb{R}^{n_\lambda} \to \mathbb{R}_+$ is the probability density of λ. Hence, $h_u^{-1}(\theta)$ is the most probable λ given that the controllable parameters are u and the observables are θ. Then we can build an approximation of the operation boundary $\partial\mathcal{S}$ by choosing different directions (u_d, θ_d) in the space where (u,θ) lives starting at some (u_0,θ_0), and following the path $\Gamma(s) = (u_0 + su_d, h^{-1}_{u_0+su_d}(\theta_0 + s\theta_d))$ until the loadability limit is reached. This can be compared to the method to build the security region suggested in [78].

An alternative is to, for each direction (u_d, λ_d), let s solve

$$\min_{s\in\mathbb{R}_+,\,\lambda\in\mathbb{R}^{n_\lambda}} \quad s, \tag{3.9a}$$

$$\text{s.t.} \quad \lambda \in \Sigma_0(u_0 + su_d), \tag{3.9b}$$

$$h(u_0 + su_d, \lambda) = \theta_0 + s\theta_d. \tag{3.9c}$$

Hence, choosing the smallest increase in a given direction in controllable parameter–observables space that may correspond to a uncertain parameter vector on the loadability limit surface.

The cost of operation

Assume that the observables during the operation period $[0,T]$ are modeled by a stochastic process $X = (X_t)_{0\le t\le T}$. The expected cost of operation during $[0,T]$, when the controllable system parameters follow the function $u : [0,T] \to U \subset \mathbb{R}^{n_u}$, can be approximated by the *operation cost functional*

$$J(u(\cdot)) = E\left[\int_0^{T\wedge\tau_{\mathcal{S}}} \{f(t, X_t^u, u(t)) + C_G(u(t))\}\,\mathrm{d}t + \mathbb{1}_{\{\tau_{\mathcal{S}}\le T\}} g(\tau_{\mathcal{S}}, X^u_{\tau_{\mathcal{S}}}, u(\tau_{\mathcal{S}}))\right], \tag{3.10}$$

where $(X_t^u)_{0\leq t\leq T}$ is the result of applying the control u to X, $\tau_{\mathcal{S}} = \inf\{t > 0 : (u(t), X_t^u) \notin \mathcal{S}\}$ is the first time that the observables reach the operation boundary, $g : [0,T] \times \mathbb{R}^k \times \mathbb{R}^{n_u} \to \mathbb{R}_+$ is the expected cost when this happens and $C_G : U \to \mathbb{R}$ is the cost, per time unit, of the control.

In the next chapter we consider finding the u that minimizes $J(u(\cdot))$ when X is a Markov process and u is only allowed to take a specific form that corresponds to controlling the power flow through the regulating market.

Remark Note that we distinguish between the cost of reaching the operation boundary after a contingency and in non-contingency state. While the former induces a cost in f through $C_{f,2}$, the latter is represented by the function g.

Chapter 4

The stochastic control approach to optimal activation of regulating bids

In this chapter we present an overview of our stochastic control based approach to power system operation which is the main contribution of the thesis. We make comparisons and discuss differences to earlier research devoted to applications in mathematical finance. This chapter serves as a prelude to Articles VI–VIII. Short introductions and comments to these articles are given at the end of the chapter.

At the end of the previous chapter we saw how the operation cost for the time period $[0, T]$ can be approximated by an integral including a control u and a stochastic process X. To optimize operation we would like to choose u to minimize the operation cost functional $J(u(\cdot))$ as defined by (3.10). To satisfy the limitations in the way generation is controlled we have to put some restrictions on the control u. When optimizing operation of the tertiary control by optimizing the activation of regulating bids, u can be seen as the result of a sequence of impulses, where each impulse corresponds to the activation of a bid. This restriction of u leads to an impulse control problem with delayed reaction [79]. Using dynamic programming we will transform our impulse control problem to a sequence of interconnected optimal stopping problems.

In the first section of this chapter we give an introduction to optimal stopping of Markov processes. Then in Section 4.2 an informal definition of impulse control problems is given along with a description of how an impulse control problem is transformed into an iterated sequence of optimal stopping problems. The reason for starting with optimal stopping is that this gives a natural introduction to stochastic control which will make it easier to understand the impulse control problem later. In Section 4.3 we describe how our problem can be interpreted as an impulse control problem. One of the main challenges with our problem is that after the activation

of a bid the following reaction is delayed. Impulse control problems with delayed reaction are known to be technically cumbersome. In Section 4.4, we discuss implications of delayed reaction in stochastic control problems and how delayed reaction can be approximated.

4.1 Optimal stopping of Markov processes

The theory of optimal stopping is concerned with the problem of choosing a time to take a particular action in order to maximize an expected reward, or minimize an expected cost. We start by giving a simple example of an optimal stopping problem.

Example 4.1 On Thursday morning on the second last week of summer Kalle is just about to lose one of his front teeth. For each lost tooth Kalle's father pays him 15 SEK. For 15 SEK Kalle can buy three ice-creams for 5 SEK a piece from the ice-cream truck that comes every Thursday afternoon. However, the ice-cream truck only comes in the summer and after that Kalle has to go to the kiosk where 15 SEK only gives him one ice-cream.

Now, Kalle's father gives Kalle the option to sell his tooth while it is still in his mouth, for 10 SEK. When should Kalle exercise the option and how much is the option worth if the probability is 0 that he loses the tooth that Thursday, 0.5 that he loses the tooth before the ice-cream truck comes next Thursday and 0.5 that it will come loose after that?

In this example Kalle has three choices. He can take 10 SEK today and buy two ice-creams. He can wait until next week and exercise the option if the tooth is still in his mouth by then or he can chose not to exercise the option at all.

If the tooth is not out by next Thursday the last option will give one ice-cream, while the second will give him two ice-creams.

Hence, if the tooth is not out by next Thursday he should exercise the option.

The expected number of ice-creams when using the option optimally next Thursday is thus $3 \cdot 0.5 + 2 \cdot 0.5 = 2.5$.

If he exercises today he will get two ice-creams. Hence, the optimal strategy is to wait until next Thursday and sell the tooth then (independent of weather it is in his mouth or not) as this gives an average of 2.5 ice-creams. Since the expected number of ice-creams without the option equals 2, the option is worth 0.5 ice-creams. Figure 4.1 gives a schematic sketch of the optimal control. □

Example 4.1 is an example of a discrete time optimal stopping problem. The approach of starting at the last exercise date (next Thursday) and computing the optimal value there and then comparing that value to the value of exercising the next to last date (this Thursday) is called the dynamic programming approach.

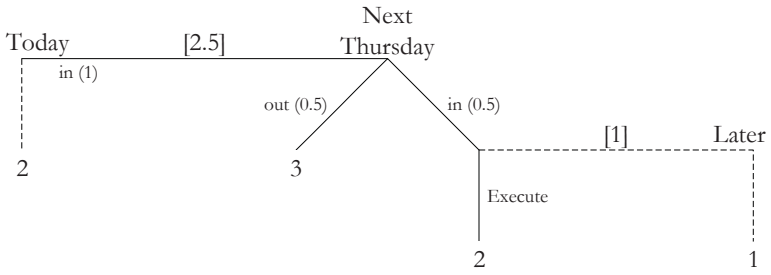

Figure 4.1: A sketch of the optimal control in Example 4.1.

Let $X = (X_j)_{j=0}^N$ be a Markov process taking values in $\mathbb{R}^k$ and let $f : \{0, \dots, N-1\} \times \mathbb{R}^k \to \mathbb{R}$ and $g : \{0, \dots, N\} \times \mathbb{R}^k \to \mathbb{R}$ be two functions. An optimal stopping problem for the process X is to find a stopping time τ^* (called an optimal stopping time) taking values in $\{0, \dots, N\}$ and the corresponding value function

$$V^*(x) = E\left[\sum_{j=0}^{\tau^*-1} f(j, X_j) + g(\tau^*, X_{\tau^*}) \Big| X_0 = x\right], \tag{4.1}$$

for which

$$V^*(x) \geq E\left[\sum_{j=0}^{\tau-1} f(j, X_j) + g(\tau, X_\tau) \Big| X_0 = x\right], \tag{4.2}$$

for all other stopping times τ. A stopping time for X is a finite random variable that does not depend on information from the future. Hence, for a stopping time the event $\{\tau \leq t\}$ only depends on the information available at time t, *i.e.* the path of X up to time t in this case. This is referred to as stopping times being *non-anticipative* [80].

There are two main approaches to solving optimal stopping problems, the maximum principle [80], and the dynamic programming approach [81].

The dynamic programming approach is based on starting at time N, and defining $S_N = g(N, X_N)$. We then move backward in time by letting

$$S_n = \max\left\{g(n, X_n), f(n, X_n) + E\left[S_{n+1} \big| X_n\right]\right\}. \tag{4.3}$$

This gives a solution to the optimal stopping problems with $V^*(x) = S_0 \big| \{X_0 = x\}$ and

$$\tau^* = \inf\{0 \leq k \leq N : S_k = g(k, X_k)\}. \tag{4.4}$$

The sequence $(\sum_{j=0}^{n-1} f(j, X_j) + S_n)_{n=0}^N$ is often referred to as the *Snell envelope* for the optimal stopping problem.

Numerical solution

The dynamic programming principle provides a straightforward way to obtain numerical solutions to optimal stopping problems. The main challenge when implementing the dynamic programming approach is to compute the conditional expectations in (4.3). One way of doing this that seems to work particularly well for problems of high dimension is the least-squares Monte Carlo method proposed by Longstaff and Schwartz in [82]. In their algorithm, which we will refer to as the LS-algorithm, a large number of paths $(x^i)_{i=1}^{N_p}$ are generated from the distribution of X. Using this sequence the authors start from the back and use least-squares to approximate the coefficients c_j^n so that, for each n,

$$E\left[S_{n+1}\middle|X_n\right] \approx \sum_{j=1}^{M^\#} c_j^n \chi_j(X_n), \tag{4.5}$$

where $\{\chi_j\}_{j=1}^{M^\#}$ is a sequence of basis functions. The great insight of [82], compared to the earlier method of Tsitsiklis and van Roy [83,84], was that it is better to keep track of the optimal strategy of stopping after time n, rather than to use the already computed approximation of $E\left[S_{n+2}\middle|X_{n+1}\right]$ when approximating c_j^n, as this could induce an error that accumulates over iterations. We will refer to the method by Tsitsiklis and van Roy as the TvR-algorithm.

Example 4.2 Assume that $(X_t, 0 \leq t \leq T)$ is a continuous time Markov process representing the time fluctuation of the price of some commodity. An American put option for this commodity with strike price K and expiry date T gives the holder the opportunity to at any time in the interval $[0, T]$ obtain the difference between the strike price and the value of the commodity, *i.e.* $K - X_t$. To value the option we need to find the exercise strategy (optimal stopping time) that maximizes the income for the holder of the option. We will do this by moving to discrete time and approximating the optimal stopping time with a stopping time taking values in the discrete time set.

Assume that $T = 3$, the initial price of the commodity is $X_0 = 1$, the risk-less interest rate is 5% and the strike price is $K = 1.10$. To price the option we will use a discretization with four time-points $\{0, 1, 2, 3\}$ and try to find the stopping time taking values in $\{0, 1, 2, 3\}$ that maximize

$$E\left[e^{-r\tau}(K - X_\tau)^+\right], \tag{4.6}$$

where $r = 0.05$ is the risk-less interest rate. Hence, we have an optimal stopping problem with $f \equiv 0$ and $g(t, x) = e^{-rt}(K - x)^+$. Here, $a^+ = \max(a, 0)$.

Assume that we wish to estimate the value of the option using the seven paths of X_t given in Table 4.1.

The corresponding discounted payoffs when exercising at the different times are given in Table 4.2.

Table 4.1: Price of the commodity.

Path	t=0	t=1	t=2	t=3
1	1.00	1.02	0.97	1.03
2	1.00	0.99	0.96	0.98
3	1.00	1.06	1.08	1.07
4	1.00	0.96	0.94	0.92
5	1.00	1.08	1.10	1.14
6	1.00	1.01	0.98	1.00
7	1.00	0.98	0.92	0.97

Table 4.2: The discounted payoffs.

Path	t=0	t=1	t=2	t=3
1	0.1000	0.0761	0.1176	0.0602
2	0.1000	0.1046	0.1267	0.1033
3	0.1000	0.0380	0.0181	0.0258
4	0.1000	0.1332	0.1448	0.1549
5	0.1000	0.0190	0	0
6	0.1000	0.0856	0.1086	0.0861
7	0.1000	0.1141	0.1629	0.1119

If not already exercised at time $t = 3$, the holder of the option will obtain the payoff for $t = 3$. Hence, the last column in Table 4.2 represents S_3.

To find S_2 we need to compute $E\left[S_3 \middle| X_2\right]$. Table 4.3 shows the data for X_2 and S_3 on which regression is to be applied. Here, the fifth path has been omitted

Table 4.3: Data for computing V_2.

Path	X_2	S_3
1	0.97	0.0602
2	0.96	0.1033
3	1.08	0.0258
4	0.94	0.1549
5	—	—
6	0.98	0.0861
7	0.92	0.1119

since it is never optimal to exercise a path that is not "in the money". We will use three basis functions $\chi_1(x) = 1$, $\chi_2(x) = x$ and $\chi_3(x) = x^2$. Using least-squares

regression on the data with this basis gives

$$E\left[S_3\middle|X_2\right] = 2.4736 - 4.1315 \cdot X_2 + 1.7257 \cdot (X_2)^2 =: V_2(X_2). \tag{4.7}$$

A graphical illustration of the estimate is given in Figure 4.2.

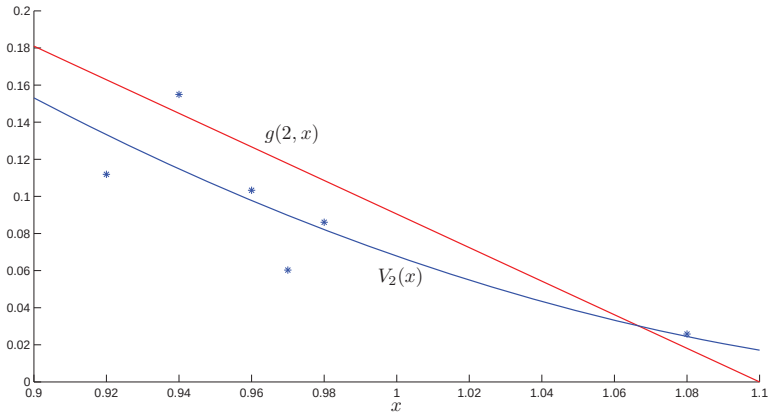

Figure 4.2: Comparing $g(2,\cdot)$ and $V_2(\cdot)$.

Assume that the holder has not yet exercised the option at time $t = 2$. If $V_2(X_2) > g(2, X_2)$ the regression estimate of the expected payoff when not exercising at time $t = 2$ is greater than the payoff when exercising. Hence, in this case the holder should not exercise the option. If, on the other hand, $V_2(X_2) \leq g(2, X_2)$ she should exercise the option at time $t = 2$.

As pointed out earlier, to create samples of S_2 it is better to take $S_2 = S_3$ for the samples with $V_2(X_2) > g(2, X_2)$ and let $S_2 = g(2, X_2)$ otherwise (LS-algorithm), rather than to set $S_2 = \max(V_2(X_2), g(2, X_2)))$ (as in the TvR-algorithm). Hence, for paths 1,2,4,6 and 7 the holder should exercise the option at time $t = 2$ and we set $S_2 = g(2, X_2)$. For paths 3 and 5 the holder should not exercise the option at time $t = 2$ and instead we get $S_2 = S_3$.

We thus obtain the values for S_2 of Table 4.4. Proceeding as above we get

$$E\left[S_2\middle|X_1\right] = -7.9835 + 17.1848 \cdot X_1 - 9.0731 \cdot (X_1)^2 =: V_1(X_1). \tag{4.8}$$

Now, we just repeat the same procedure to get the samples of S_1 in Table 4.5. Since we always start with $X_0 = 1.00$ the holder either immediately exercises the option and gets 0.10 or she waits at least until time $t = 1$ and get on average $E[S_1] = 0.1025$. Since the expected value of waiting is larger, the holder should not exercise the option at time $t = 0$, and the value of the option is 0.1025.

From (4.4) we get the following discrete time approximation of τ^*,

$$\bar{\tau}^* = \inf\{j \in \{1, 2, 3\} : V_j(X_j) \leq e^{-rj}(K - X_j)^+\}, \tag{4.9}$$

which is the earliest optimal stopping time for the problem. □

Table 4.4: Data for computing V_1.

Path	X_1	S_2
1	1.02	0.1176
2	0.99	0.1267
3	1.06	0.0258
4	0.96	0.1448
5	1.08	0
6	1.01	0.1086
7	0.98	0.1629

Table 4.5: Our seven samples of S_1.

Path	S_1
1	0.1176
2	0.1267
3	0.0380
4	0.1448
5	0.0190
6	0.1086
7	0.1629

4.2 Impulse control

An impulse control is a sequence $v = (\tau_1, \tau_2, \ldots; \xi_1, \xi_2, \ldots)$, where $\tau_1 \leq \tau_2 \leq \cdots$ are stopping times (called intervention times), and $\xi_1, \xi_2 \ldots$ are the corresponding impulses (called interventions). Here, for obvious reasons, the ξ_i are only allowed to be decided using information available at the corresponding intervention times τ_i. The interventions are often in some way limited, *e.g.* we cannot sell more stocks than we own, so that $\xi_j \in I$ for some interval I. Impulse control problems have many applications such as natural resource extraction [85], optimal investment policies [86] and optimal portfolio selection [87].

An impulse control problem for the Markov process X_t, taking values in $\mathbb{R}^k$, can be to find the strategy v^* that maximize

$$E\left[\int_0^{\tau_{\mathcal{S}}} f(s, X_s^v)\,\mathrm{d}s + g(\tau_{\mathcal{S}}, X_{\tau_{\mathcal{S}}}^v) + \sum_{\tau_j < \tau_{\mathcal{S}}} K(\tau_j, \xi_j)\right] \tag{4.10}$$

and calculate the corresponding optimal value. Here, X_t^v is a stochastic process, that depends on the control v. For example, we can set $X_t^v = X_t - \sum_{j=1}^{\infty} \mathbb{1}_{\tau_j \leq t} \xi_j$. The terminal time $\tau_{\mathcal{S}}$ is typically of the form

$$\tau_{\mathcal{S}} = T \wedge \inf\{t > 0 : X_t^v \notin \mathcal{S}\}, \tag{4.11}$$

for some domain $\mathcal{S} \subset \mathbb{R}^k$ and some given time $T > 0$. If $T < \infty$ the problem is said to be of finite horizon.

An example is if X_t^v is the value of our share of a stock and we want to optimize selling for a specific time period $[0, T]$ or until bankruptcy at $X_t^v = 0$, *i.e.* $\mathcal{S} = (0, \infty]$. The rate function $f : [0, T] \times \mathbb{R}^k \to \mathbb{R}$ will then represent the dividends and $g : [0, T] \times \mathbb{R}^k \to \mathbb{R}$ the discounted terminal value of our share of the stock. The implied gain of an impulse $K : [0, T] \times \mathbb{R} \to \mathbb{R}$ will in this case be the revenue from selling stocks and $\xi_j \in (0, X_{\tau_j}^v]$.

Impulse control as iterated optimal stopping

If we limit the number of interventions to be no more than $N < \infty$ it is possible to write the impulse control problem as a sequence of iterated optimal stopping problems. Let $\Phi^j(t, x)$ be the optimal value when starting the problem afresh at time t with $X_t = x$ and j interventions remaining. Then

$$\Phi^j(t,x) = \sup_\tau E\left[\int_t^\tau f(s, X_s^v)\,\mathrm{d}s + \sup_{\xi \in I}\left\{K(\tau,\xi) + \Phi^{j-1}(\tau, X_\tau - \xi)\right\}\Big| X_t = x\right].$$

Hence, by exploiting the Markovian nature of the problem we can, by solving an iterated sequence of optimal stopping problems, find the value function with any finite number of interventions remaining. Using the Snell envelope formulation of optimal stopping times we get the intervention times as,

$$\tau_i = \inf\{t \geq \tau_{i-1} : \Phi^{N-i}(t, X_t) = \mathcal{M}^{N-i}(t, X_t)\},$$

where

$$\mathcal{M}^j(t,x) = \sup_{\xi \in I}\left\{K(t,x) + \Phi^{j-1}(t, x-\xi)\right\}.$$

The corresponding interventions are given as measurable selections of

$$\xi_i \in \operatorname*{Argmax}_{\xi \in I}\left\{K(\tau_i, X_{\tau_i}) + \Phi^{N-i}(\tau_i, X_{\tau_i} - \xi)\right\}.$$

The idea of formulating impulse control problems as iterated optimal stopping problems goes back to the 1980s, see *e.g.* [88].

Optimal switching

Optimal switching problems are a special type of impulse control problems where the impulses are confined to taking values in a finite set. Optimal switching problems generally arise when trying to optimize the production in some production facility where production can only be run at a finite number of different levels and the profitability of production depends on the price of a number of commodities.

One example that was brought forward in [89–91] is that of an electricity producer trying to optimize production. It is assumed that the production in a power plant can be run at a finite number of production levels and that a cost is induced by switching between the levels. Hence, in order to optimize production in the time period $[t, T]$ starting with $X_t = x$ in state i, the power plant manager has to solve the following impulse control problem

$$V^i(t,x) = \sup_u E\left[\int_t^T \varphi_{u_s}(s, X_s)\,\mathrm{d}s - \sum_{t<\tau_j<T} C_{u_{\tau_j-},u_{\tau_j}} \big| X_t = x,\, u_t = i\right], \quad (4.12)$$

where $u = (\tau_1, \tau_2, \ldots; \xi_1, \xi_2, \ldots)$ is the impulse control, where the ξ_i takes values in the set of production states, and the supremum is taken over all such controls. Here, X_t is a k–dimensional stochastic process representing, for example, the price of electricity and the market price of uranium, $u_t = \sum_{\tau_j<T} \xi_j \mathbb{1}_{[\tau_j,\tau_{j+1})}(t)$ is the production state at time t, $\varphi_\xi(t,x) : [0,T] \times \mathbb{R}^k \to \mathbb{R}$ is the profit rate when running the power plant in state ξ at time t when the electricity price and the fuel prices are given by the vector x and $C_{i,j} > 0$ is the cost of switching from state i to state j.

In [89] the authors propose an efficient modification of the LS-algorithm to obtain a numerical solution to this problem. It is this approach that we have built on to obtain a numerical solution scheme for optimizing the activation of regulating bids.

4.3 Impulse control and activation of regulating bids

There are some obvious similarities between the power plant managers problem of maximizing the profit by switching between different production levels and the system operator's problem of optimally activating the regulating bids. The activation of a regulating bid can be considered synonymous to switching to a new production level and will induce a cost (positive for upward balancing and negative for downward balancing) to the system operator.

Assume that N bids have been handed in to the regulating market and the system operator wants to optimize the activation of regulating bids in the time interval $[0, T]$. The system operator's decisions will be based on observations of k observable system variables modeled by the k–dimensional Markov process $(X_t,\, 0 \le t \le T)$.

We assume that the activation of a regulating bid is an irreversible process so that no bid can be deactivated. As mentioned in Section 2, this is in general the case on the Nordic market [35]. The control taken by the system operator can then be represented by a sequence $v = (\tau_1, \ldots, \tau_N; \alpha_1, \ldots, \alpha_N)$. The physical interpretation of v is that bid α_j is activated at time τ_j.

We let $v_t = \{(\tau_1, \ldots, \tau_n; \alpha_1, \ldots, \alpha_n) : n = \max\{k : \tau_k \le t\}\}$ and define for all $(t,x) \in [0,T] \times \mathbb{R}^k$, $f^{v_t}(t,x) = f(t,x,u^v(t))$ and $g^{v_t}(t,x) = g(t,x,u^v(t))$, where

$u^v(t)$ is the controllable parameter values at time t corresponding to the control v_t. The minimal operation cost problem of (3.10) now takes the form

$$J^v = E\left[\int_0^{T\wedge\tau_{\mathcal{S}}} f^{v_t}(t, X_t^v)\,\mathrm{d}t + \mathbb{1}_{\{\tau_{\mathcal{S}}\le T\}} g^{v_{\tau_{\mathcal{S}}}}(\tau_{\mathcal{S}}, X_{\tau_{\mathcal{S}}}^v) + \sum_{\tau_k < T\wedge\tau_{\mathcal{S}}} K_{\alpha_k}(\tau_k)\right], \quad (4.13)$$

where $X^v = X^{u^v}$ and $(K_i : [0,T] \to \mathbb{R})_{i=1}^N$ is as defined in Section 2.4. With our assumptions the system operator's problem is thus a switching problem for which switches are only allowed to go in the direction of more activated bids.

Remark In the appended articles each term of (4.13) has been multiplied by a factor e^{λ_t} to account for removal of cases when contingencies occur.

Remark If we assume that there is always a positive cost for an activation directly followed by a deactivation of the same bid, then it is quite straightforward to generalize the impulse control problem to also allow for deactivation of bids (see [89] and references therein).

We must have that $\alpha_j \in \{1,\dots,N\} \setminus \{\alpha_1,\dots,\alpha_{j-1}\}$ since no bid can be activated more than once. The sequence of interventions $\alpha_1,\dots,\alpha_N$ will thus make up the edges of a directed graph as shown in Figure 4.3. Here, each vertex represents

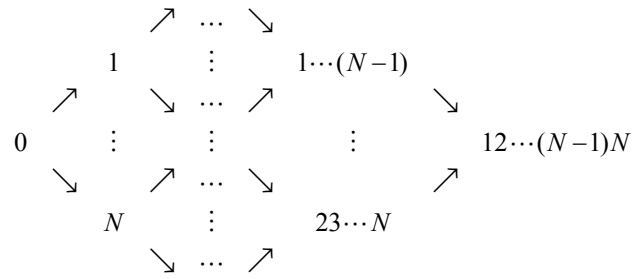

Figure 4.3: The directed graph representing the activation of regulating bids.

a set of activated bids, and each edge in the graph represents the activation of a new bid. In the nth column of the graph in Figure 4.3, there are $\binom{N}{n}$ vertices, and the total number of vertices in the graph is 2^N.

Unfortunately, the reaction times of the actors on the regulating market and the ramp rates of their power plants are important aspects that need to be considered. This will introduce a delay in the reaction of switches.

4.4 Delayed reaction

Impulse control problems with delayed reaction are known to be technically cumbersome [92]. What allowed us to formulate an impulse control problem as a sequence of iterated optimal stopping problems was the fact that the value function was Markovian. When introducing delays this is no longer the case.

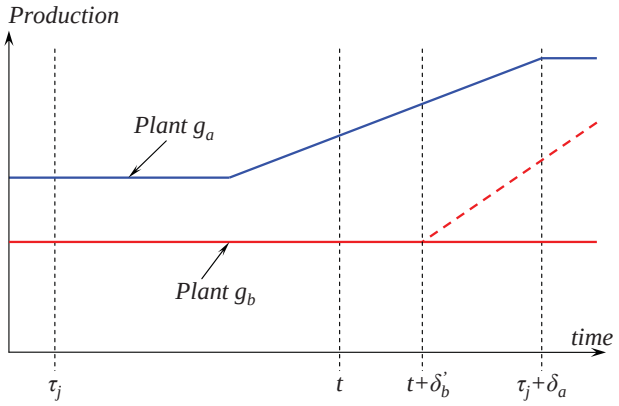

Figure 4.4: The result of delays.

Consider the situation depicted in Figure 4.4. At time τ_j the system operator activates Bid a, *i.e.* $\alpha_j = a$, which is connected to the production in power Plant g_a. The order to activate the bid is followed by a reaction time and a ramping giving a total delay between activation and execution of δ_a. A moment later, at time $t < \tau_j + \delta_a$ the system operator is considering to activate also Bid b connected to the output of Plant g_b. If activation of this bid is performed at this time, the production will ramp up starting at time $t + \delta_b' < \tau_j + \delta_a$. When making the decision the system operator has to consider the cost of operation in the time interval $[t, \tau_j + \delta_a]$, where the production in Plant g_a is a function of $t - \tau_j$ and thus depends on the activation time τ_j of Bid a.

In the literature a few different ways of approximating delays have been proposed.

In [89] it is proposed that time separation can be used to approximate switching delays. Time separation is given by prohibiting any further switches in a time period $[0, \delta)$ following every switching, *i.e.* $\tau_{j+1} \geq \tau_j + \delta_a$ in the case described above. In Figure 4.5 we show how time separation works. With time separation ramp rates are not modeled since switches are instantaneous. Instead, at time t we have to wait until time $\tau_j + \delta_a$ before activating Bid b (which will lead to an instantaneous switch of the production in Plant g_b).

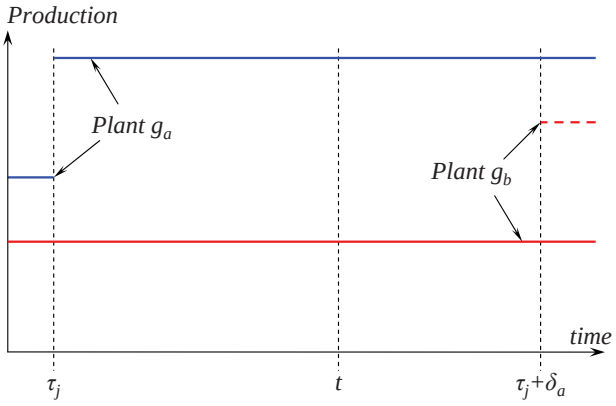

Figure 4.5: Approximated by time separation.

For obvious reasons, time separation is not a suitable approximation for the system operator's problem. We take away the reaction times and the ramp rates which are important parts of the problem and substitute these with preventing activation during some periods. Since the main goal of the system operator is to find the optimal control (and not the corresponding value function), time separation is not an appropriate choice for approximating delays in our case.

In [79] a technique similar to time separation for approximating delays in general impulse control problems is proposed. Here, the authors design an operator taking care of the delay period. This means that we can model reaction times and ramp rates accurately. However, we still have the same drawback as with time separation. With this approach we can activate several bids simultaneously, but no activation is allowed during the period between that Bid a is activated at time τ_j and executed at time $\tau_j + \delta_a$. This situation is shown in Figure 4.6. Either Bid b is activated at time τ_j, so that $\tau_{j+1} = \tau_j$ (dashed red line) or after the execution of Bid a, so that $\tau_{j+1} \geq \tau_j + \delta_a$ (dotted red line). Since, the activation times of regulating bids can sometimes be quite long (for example, up to 15 minutes in the Swedish system [35]) this approximation technique is also very limited.

It seems like there is no available method for approximating delays that provides sufficient accuracy in our case. Instead we have focused on making the value function Markovian by increasing the dimension of the state space and designing an efficient numerical solution scheme for the resulting problem. It turns out that in this case the TvR-algorithm is superior to the LS-algorithm for problems with several bids.

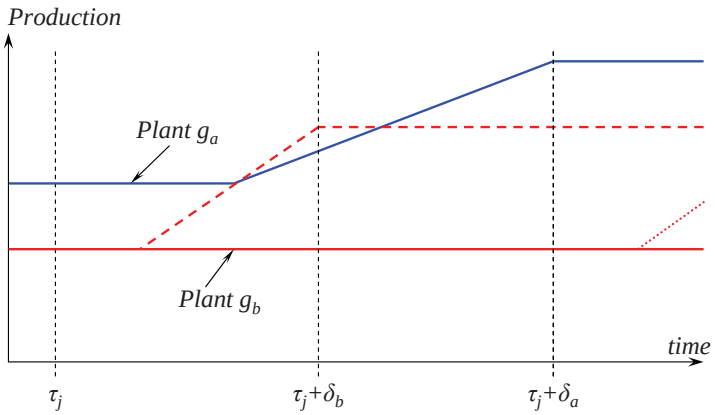

Figure 4.6: Approximated by non-overlapping interventions.

4.5 Articles

Article VI

In the first article on optimal activation of regulating bids we consider a system with one observable that is model by Brownian motion with drift. This gives us the opportunity to use analytical methods to derive the solution of the problem as the solution to a system of equations.

Article VII

In this article we focus on the power system side of the problem. The general formulation of the system operator's problem of optimizing the activation of regulating bids is presented. A solution technique based on the LS-algorithm is outlined and in a numerical example a simple two bid, two observables problem is investigated. We also numerically investigate the effect of delays on the problem by considering what will happen if delays are neglected.

Remark To make presentation more general, regulating bids are referred to as tertiary reserves in Article VII.

Article VIII

In Article VIII we consider the same problem as in the previous article but more details are provided. In this article we propose numerical solution schemes based on both the LS-algorithm and the TvR-algorithm for solving the system operator's problem. It turns out that for solving impulse control problems with delayed reaction the TvR-scheme can give much more computationally efficient results.

Article VIII is concluded with a numerical example. In this numerical example we consider the same system as in Article VII. However, here we compare the two numerical schemes to one another.

Chapter 5

Increasing Transfer Capacity

In this chapter we discuss how the physical capacity to transfer electric power can be enhanced. At the end of this chapter we give short introductions to Articles IX and X.

So far in this thesis we have only considered how to minimize operation costs by optimizing the activation of regulating bids. This optimization only concerns the risk-taking and results in an efficient NTC. The longer the system operator waits before activating a bid, the higher the risk of having a system failure will be.

Another way of making operation more efficient is to use the available system components better, and thus increase the TTC. A huge part of the literature on power system operation is concerned with this issue.

By tuning controllers in High Voltage Direct Current (HVDC) and Flexible AC Transmission System (FACTS) devises more efficiently it is possible to improve the transient stability properties of the system [93] as well as the small signal stability properties [94].

5.1 Articles

Article IX

As pointed out in Section 2.4, the distribution of the primary control gain between the plants in the system will have a strong influence on the risk of system failure. In Article IX we propose an algorithm for computing the distribution of the primary control gain that maximizes the distance from the operating point to the power flow feasibility boundary. The algorithm is based on an iterated gradient decent technique.

Article X

In Article X we consider a system that has multiple HVDC-links and compute the power modulation gain of the HVDC-links to maximize the small signal stability limit along a given load path. The computation is based on Particle Swarm Optimization (PSO). To test the method we make dynamical simulations on a system where the load follows a stochastic process.

Remark It seems that during the publication process some references to equations in this article have been redirected. Therefore, the published version of this article is not used in the thesis.

Chapter 6

Conclusions and Future Work

In this, the last chapter of the thesis, conclusions are drawn and guidelines for future work are outlined. We discuss how the methods presented in the appended articles can be improved and further developed to meet the increasing demand on efficient power system operation.

6.1 Conclusions

This thesis treats transmission limits in power system operation. The aim of the thesis is to find a method for deciding a Net Transfer Capacity (NTC) that minimizes the expected operation cost. Previous research in the area has mainly been focused at developing and investigating different methods of applying a security criterion to get the Total Transfer Capacity (TTC). From the TTC a security margin has then been subtracted to get the NTC. A security criterion typically says that the power system should always maintain stability if any l system components fail simultaneously, for some given $l \geq 1$.

In this thesis, a new way of finding operation strategies that incorporates transmission limits is proposed. The new method is not based on a security criterion. Instead we propose that a database of expected costs, with entries corresponding to different values of the controllable system parameters $u \in \mathbb{R}^{n_u}$ and a vector of observable system parameters $x \in \mathbb{R}^k$, is built. This database is preferably built using Monte Carlo simulation where contingencies can be chosen using a contingency selection technique, such as the one proposed in [43].

To build the database we propose a Markov Chain Monte Carlo technique to generate outcomes of the full set of system parameters $\lambda \in \mathbb{R}^{n_\lambda}$ given values of the controllable system parameters u and the observable system parameters x. Then a contingency can be chosen using a contingency selection technique, such as the one proposed in [43]. For each contingency not leading to immediate system failure we analyze the probability that post-contingency corrective rescheduling can be used

to keep the system from losing stability. For this both a deterministic and a Monte Carlo scheme were developed.

Once the database of expected costs is built we propose a numerical scheme for estimating the optimal strategy for activation of regulating bids on the regulating power market. The numerical scheme is based on the least-squares Monte Carlo method developed by Tsitsiklis and van Roy [83, 84].

Another way of improving the efficiency of the system is by increasing the physical transfer capacity of the system. Two methods for this are proposed in this thesis. First we propose an adaptive rescheduling technique for the primary control. Then we investigate how coordination of HVDC devices can improve the small signal stability properties of the system.

6.2 Future work

The work presented in this thesis is a novel approach to include transfer limits in power system operation. When trying to answer the questions posed in the introduction we only scrape the surface on some issues. There are, therefore, many possible steps for future research some of which are listed below:

Net consumption model

Using a Gaussian process to model power consumption provides a reasonable approximation to the aggregate behavior of power consumption. Wind power production, however, is known to have a typically non-Gaussian behavior. With a large penetration of wind power the Ornstein-Uhlenbeck process proposed in the thesis is thus not an appropriate model of the net power consumption.

The Alberta Electric System Operator (AESO) publishes both wind power production and power consumption data from the Alberta power system sampled with 10-minute intervals [95]. This data can be used both to estimate parameters for a consumption model and when developing a stochastic model of wind power production.

Estimating the probability of system failure

The approach to estimate the probability, and indirectly the cost, of system failure proposed in this thesis suffers from one main weakness. No variance reduction technique is proposed for the injected powers in the MCMC simulation. Using crude Monte Carlo may be very inefficient here. Including, for example, importance sampling in the MCMC simulation would thus be preferable.

Database for expected costs

One disadvantage of using a database to store the expected costs is that as the number of observables increases the size of the database will grow out of proportion.

Assume for example that $k = 10$ and that every dimension should be partitioned into a grid of 30 elements. Then the number of entries in the database is $30^{10} \approx 6 \cdot 10^{14}$. If the estimates of the expected costs are stored in floating-point precision, this will lead to a database with a size of approximately 2360 Tb (Terabyte).

The above calculation is only for the base case generation, when planned production is constant throughout the entire time period. For a large number of observables the method will thus be impossible to implement.

Hence, some type of approximation is necessary. What seems best here is to use a series expansion to approximate the estimates of the expected costs (as in the LS- and the TvR-algorithms). We can put

$$f(u, x) = \sum_{j=0}^{N_B} c_j \chi_j^f(u, x),$$

where $\chi_j^f : \mathbb{R}^{n_u} \times \mathbb{R}^k \to \mathbb{R}$ are basis functions and N_B is the number of basis functions.

This was how Example 2 in Article VII was solved. However, before we are ready to accept such an approximation we first need to test, on a smaller system, if the method is robust to approximation errors in the cost rate function and analyze what shape the functions χ_j^f should take.

Another advantage of using a series expansion to represent the expected cost from failures is that we do not need to take the detour around MCMC. Instead we can generate outcomes of the injected powers, calculate the corresponding values of the observables and estimate the corresponding probability of failure, and cost of failure. When this have been repeated enough times we simply use least-squares to approximate the coefficients c_j in the above formulation. This will make it more simple to use importance sampling to generate samples of the loads.

Absolute operation boundaries

By the same reasons as above, approximating the absolute operations boundary becomes necessary when the number of observables increases. Here, as with the loadability limit surface in parameter space, using a local approximation seem suitable.

Including AGC in the optimization

To include AGC in the problem to minimize the operation cost (3.10) we need to add to u^v a control corresponding to the continuously changing output of the n_{AGC} power plants where the generation is controlled by the AGC system. If we let $u(t, v, w) = u_2^w(t) + u_3^v(t)$, where $u_3^v = u^v$ is the tertiary control as defined in

Section 4.3 and

$$\begin{aligned} \dot{u}_2^w(t) &= b(t, u_2^w(t), w(t)), \quad \forall t \in [0,T] \\ u_2^w(0) &= u_0^w. \end{aligned}$$

with the control constraint

$$w(t) \in W \subset \mathbb{R}^{n_{\text{AGC}}}, \quad \forall t \in [0,T]$$

and the state constraint

$$u_2^w(t) \in U_w \subset \mathbb{R}^{n_u}, \quad \forall t \in [0,T].$$

Here, $b : [0,T] \times \mathbb{R}^{n_{\text{AGC}}} \times W \to \mathbb{R}^{n_{\text{AGC}}}$ is a smooth function representing, for example, the rate at which the power plants in the AGC change their production.

The control constraint is included so that maximal ramp rates of power plants are not violated by the control, and the state constraints are there to limit the total production so that it does not exceed the installed capacity and to limit the minimal production in the different power plants.

The system operators cost minimization problem is now to minimize $J(u(\cdot, v, w))$ by choosing an optimal pair (v, w) where v is an impulse control of the type described in Section 4.3 and w is a ($\mathcal{F}_t$–measurable) control which fulfills the constraints listed above.

Solution by stochastic maximum principle

The methods used to solve the impulse control problems in the articles appended to this thesis are all based on the dynamic programming principle. Another approach for solving stochastic control problems is to use the stochastic maximum principle. With the stochastic maximum principle the solution to the stochastic control problem for a diffusion process is obtained as a system of forward-backward stochastic differential equations (FBSDEs) [80, 96]. This approach could make computation much more efficient.

Assume that we have a control $u : [0,T] \to U \in \mathbb{R}^{n_u}$, which controls the stochastic process X^u defined by a stochastic differential equation (SDE) driven by a m–dimensional Brownian motion W as

$$\begin{aligned} \mathrm{d}X_t^u &= b(t, X_t^u, u_t)\,\mathrm{d}t + \sigma(t, X_t^u)\,\mathrm{d}W_t, \quad t \in [0,T]; \\ X_0 &= x_0. \end{aligned}$$

Assume now that we wish to find the non-anticipative control u that minimizes

$$J(u) = E\left[\int_0^T f(t, X_t^u, u_t)\,\mathrm{d}t + g(X_T^u)\right].$$

In this problem it is assumed that $b : [0,T] \times \mathbb{R}^k \times U \to \mathbb{R}^k$, $\sigma : [0,T] \times \mathbb{R}^k \to \mathbb{R}^{k \times m}$, $f : [0,T] \times \mathbb{R}^k \times U \to \mathbb{R}$ and $g : \mathbb{R}^k \to \mathbb{R}$ all satisfy some given conditions on regularity (see S0-S3 on page 114 of [80]).

Let $\hat{u}$ be the optimal control to this problem and set $\hat{X} = X^{\hat{u}}$. The *adjoint equation* to the problem is

$$\begin{aligned} \mathrm{d}Y_t = &-\big[b_x(t,\hat{X}_t,\hat{u}_t)Y_t + \sum_{j=1}^{m} \sigma_x^j(t,\hat{X}_t)^\top (Z_t)_j - f_x(t,\hat{X}_t,\hat{u}_t)\big]\,\mathrm{d}t + Z_t\,\mathrm{d}W_t, \\ &\qquad\qquad t \in [0,T]; \\ Y_T = &-g_x(\hat{X}_T), \end{aligned}$$

which is a backward stochastic differential equation (BSDE) with a pair of unknowns (Y,Z). Here, Y_t takes values in $\mathbb{R}^k$ and Z_t takes values in $\mathbb{R}^{k \times m}$. The *Hamiltonian* of the problem is defined as

$$H(t,x,u,y,z) = \langle y, b(t,x,u)\rangle + \operatorname{tr}\left[z^\top \sigma(t,x)\right] - f(t,x,u).$$

From the Hamiltonian the optimal control $\hat{u}$ can be calculated as

$$H(t,\hat{X}_t,\hat{u}_t,Y_t,Z_t) = \max_{u \in U} H(t,\hat{X}_t,u,Y_t,Z_t).$$

The adjoint variable Y_t is the *marginal value* of the asset X_t, and is some times also referred to as the *shadow price*. The maximum principle can be described as "minimizing the total cost amounts to maximizing the total contribution of the marginal values" [80].

In [97] a stochastic maximum principle for a problem involving a continuous control combined with an impulse control is derived, and in [98] a duality relation between delayed SDEs and something they call anticipated BSDEs is found. Combining the theories developed in these two articles it may be possible to solve also our problem, with AGC, using the stochastic maximum principle.

Bibliography

[1] M. Perninge, M. Amelin, and V. Knazkins. Monte carlo analysis of the trade-off between trading and security in a two-area system. In *GMSARN (The Greater Mekong Subregion Academic and Research Network) International Conference 2007, Pattaya Thailand*, 2007.

[2] M. Perninge, M. Amelin and V. Knazkins. Comparing Variance Reduction Techniques for Monte Carlo Simulation of Trading and Security in a Three-Area Power System. In *Proceedings IEEE PES T&D LA 2008*, August 2008.

[3] M. Perninge, M. Amelin, and V. Knazkins. Load modeling using the Ornstein-Uhlenbeck process. In *IEEE PECON 2008, Johor Bahru Malaysia*, 2008.

[4] M. Perninge. Modeling the uncertainties involved in net transmission capacity calculation. Technical report, Royal Institute of Technology (KTH), April 2009. Licentiate Thesis.

[5] M. Perninge, M. Amelin, and V. Knazkins. The impact of a given trading limit on a two-area test system. In *Proceedings IEEE Power Tech*, 2009.

[6] M. Olsson, M. Perninge, and L. Söder. Simulation of real-time balancing power demands in power systems with wind power. *Electric Power Systems Research*, 80:966–974, 2010.

[7] M. Perninge, V. Knazkins, M. Amelin, and L. Söder. Risk estimation of critical time to voltage instability induced by saddle-node bifurcation. *IEEE Transactions on Power Systems*, 25(3):1600–1610, 2010.

[8] M. Perninge, V. Knazkins, M. Amelin, and L. Söder. Estimating upper confidence bounds of electric power consumption. In *MEPCON*, 2009.

[9] M. Perninge and L. Söder. A probabilistic distance to the power system secure operation boundary. In *Symposium- Bulk Power System Dynamics and Control - VIII (IREP)*, 2010.

[10] M. Perninge and L. Söder. Analysis of transfer capability by markov chain monte carlo simulation. In *PECon*, 2010.

[11] M. Perninge and L. Söder. Geometric properties of the loadability surface at SNB-SLL intersections and tangential intersection points. In *ISAP*, 2011.

[12] Nordel. Principles for determining the transfer capacity in the Nordic power market. Technical report, Nordel, Jan 2008.

[13] A. J. Wood and B. F. Wollenberg. *Power Generation, Operation, and Control*. Wiley, New York, 2nd edition, 1996.

[14] J. Machowski, J. W. Bialek, and J. R. Bumby. *Power system dynamics: Stability and Control*. Wiley, second edition, 2008.

[15] Nordel. Proposed principles for common balance management, November 2007.

[16] Y. Kataoka. A Probabilistic Nodal Loading Model and Worst Case Solutions for Electric Power System Voltage Stability Assessment. *IEEE Transactions on Power Systems*, 18(4), Nov 2003.

[17] T. Van Cutsem and C. D. Vournas. *Voltage Stability of Electric Power Systems*. Kluwer Academic Publishers, 1998.

[18] R. Billinton and W. Li. *Reliability Assessment of Electrical Power Systems Using Monte Carlo Methods*. Kluwer, 1994.

[19] IEEE/CIGRE Joint Task Force on Stability Terms and Definitions. Definition and classification of power system stability. *Power Systems, IEEE Transactions on*, 19(3):1387–1401, 2004.

[20] A. R. Bergen and V. Vittal. *Power Systems Analysis*. Prentice-Hall, New Jersey, 2000.

[21] Carson W. Taylor. *Power System Voltage Stability*. Mcgraw-Hill, 1993.

[22] P. Kundur. *Power System Stability and Control*. McGraw-Hill Inc, 1993.

[23] W. Rudin. *Principles of Mathematical Analysis*. McGraw-Hill, USA, third edition, 1976.

[24] M. A. Pai. *Energy Function Analysis for Power System Stability*. Kluwer Academic, 1989.

[25] K. T. Alligood, T. D. Sauer, and J. A. Yorke. *CHAOS: An Introduction to Dynamical Systems*. Springer, New York, 1996.

[26] C. A. Cañizares, F. L. Alvarado, C. L. DeMarco, I. Dobson, and W. F. Long. Point of collapse and continuation methods for large AC/DC systems. *IEEE Transactions on Power Systems*, 8(1), Februari 1993.

[27] H. D. Chiang and F. F. Wu. Stability of nonlinear systems described by a second-order vector differential equation. *IEEE Trans. Circuits and Systems*, 35(6):703–711, 1988.

[28] E. H. Abed and P. P. Varaiya. Nonlinear oscillations in power systems. *Int. J. Elec. Power Syst.*, 6:37–43, 1984.

[29] I. Dobson and H.D. Chiang. Towards a theory of voltage collapse in electric power systems. *Systems & Control Letters*, 13(3):253 – 262, Sept 1989.

[30] I. Dobson, T. Van Cutsem, C. Vournas, C.L. DeMarco, M. Venkatasubramanian, T. Overbye, and C.A. Cañizares. Voltage stability assessment: Concepts, practices and tools. Technical report, IEEE Power Engineering Society Power System Stability Subcommittee Special Publication, 2002.

[31] European energy exchange.

[32] PJM. Scheduling operations. PJM Manual 11:, 2007.

[33] National Grid Electricity Transmission plc. The grid code, 2008.

[34] M. Olsson. *On optimal hydropower bidding in systems with wind power.* PhD thesis, KTH, 2009.

[35] Balansansvarsavtal 2011 (Swedish). Technical report, Svenska Kraftnät, 2010.

[36] ISO New England Inc. Market operations, April 2006.

[37] National Electricity Market Management Company (NEMMCO). Operating procedure: Frequency control ancillary services, July 2005.

[38] ETSO. Current state of balance management in europe, December 2003.

[39] S. Hallia. Strategi för utvecklande av reglerbud (Swedish). Technical report, KTH, 2008.

[40] Procedures for cross-border transmission capacity assessment. Technical report, European Transmission System Operators Association (ETSO), 2001.

[41] Transmission Transfer Capability Task Force. Available transmission capability definitions and determination. Technical report, North American Reliability Council, Princeton, New Jersey, June 1996.

[42] Q. Chen and J.D. McCalley. Identifying high risk $N - k$ contingencies for online security assessment. *IEEE Trans. Power Systems*, 20(2):823–834, 2005.

[43] F. Belmudes, D. Ernst, and L. Wehenkel. Cross-entropy based rare-event simulation for the identification of dangerous events in power systems. In *the 10th International Conference on Probabilistic Methods Applied to Power Systems (PMAPS-08)*, 2008.

[44] Svensk energi. Power situation in Sweden. Technical report, 2009.

[45] Nordel. Nordic grid code 2007, January 2007.

[46] www.svk.se.

[47] M. Rostami. Analysis of voltage stability calculations on the Swedish grid. Master's thesis, Royal Institute of Technology (KTH), may 2009. (in Swedish).

[48] I. Dobson, S. Greene, R. Rajaraman, C. L. DeMarco, F. L. Alvarado, M. Glavic, J. Zhang, and R. Zimmerman. Electric power transfer capability: concepts, applications, sensitivity and uncertainty. Technical report, Power Systems Engineering Research Center (PSERC), 2001.

[49] F. Capitanescu, M. Glavic, D. Ernst, and L. Wehenkel. Contingency filtering techniques for preventive security-constrained optimal power flow. *Power Systems, IEEE Transactions on*, 22(4):1690 –1697, 2007.

[50] A. Monticelli, M. V. F. Pereira, and S. Granville. Security-constrained optimal power flow with post-contingency corrective rescheduling. *Power Systems, IEEE Transactions on*, 2(1):175 –180, 1987.

[51] C. L. DeMarco. Control structures for competitive, marked-driven power systems. In *40th IEEE Conference on Decision and Control*, 2001.

[52] D. Ernst, D. Ruiz-Vega, M. Pavella, P.M. Hirsch, and D. Sobajic. A unified approach to transient stability contingency filtering, ranking and assessment. *Power Systems, IEEE Transactions on*, 16(3):435 –443, August 2001.

[53] Allan Gut. *Probability: A Graduate Course*. Springer, 2005.

[54] L.H. Sanabria and T.S. Dhillion. Stochastic power flow using cumulants and von mises functions. *Int. J. Electric Power and Energy Systems*, 8:47–60, 1986.

[55] E. A. Cornish and R. A. Fisher. The percentile points of distributions having known cumulants. *Technometrics*, 14:209–226, 1960.

[56] G. L Viviani and G. T. Heydt. Stochastic optimal energy dispach. *IEEE Transactions on Power Apparatus and Systems*, PAS-100(7):3221–3228, 1981.

[57] M. Madrigal, K. Ponnambalam, and V.H. Quintana. Probabilistic optimal power flow. *IEEE Transactions on Power Systems*, 1:385–388, 1998.

[58] A. Schellenberg, W. Rosehart, and J. Aguado. Introduction to cumulant-based probabilistic optimal power flow (P-OPF). *IEEE Transactions on Power Systems*, 20:1184–1186, 2005.

[59] A. Schellenberg, W. Rosehart, and José Aguado. Cumulant-based probabilistic optimal power flow (P-OPF) with gaussian and gamma distributions. *IEEE Transactions on Power Systems*, 20(2):773–781, 2005.

[60] G. Verbic and C. A. Cañizares. Voltage stability constrained OPF market models considering N–1 contingency criteria. *IEEE Transactions on Power Systems*, 21:1883–1893, 2006.

[61] X. Li, Y. Li, and S. Zhang. Analysis of probabilistic optimal power flow taking account of the variation of load power. *IEEE Transactions on Power Systems*, 23:992–999, 2008.

[62] M. Sobierajski. Optimal stochastic load flows. *Electrical Power Systems Research*, 2:71–75, 1979.

[63] A. O. Ekwue and R. N. Adams. Optimal power rescheduling for system security using stochastic second-order load flow. *Int. J. Elec. Power Syst.*, 11(4):277–282, 1989.

[64] A. Schellenberg, W. Rosehart, and J. Aguado. Cumulant based stochastic optimal power flow (S-OPF) for variance optimization. In *IEEE Power Engineering Society General Meeting*, 2005.

[65] H. Zhang and P. Li. Probabilistic analysis for optimal power flow under uncertainty. *IET Gener. Transm. Distrib.*, 4(5):556–561, 2010.

[66] C. D. Vournas, M. Karystianos, and N. G. Maratos. Bifurcation points and loadability limits as solutions of constrained optimization problems. In *Power Engineering Society Summer Meeting, 2000. IEEE*, 2000.

[67] Y. Kataoka and Y. Shinoda. Voltage stability limit of electric power systems with generator reactive power constraints considered. *IEEE Transactions on Power Systems*, 20:951–962, 2005.

[68] V. Ajjarapu and C. Christy. The continuation power flow: A tool for steady state voltage stability analysis. *IEEE Transactions on Power Systems*, 7(1), August 1992.

[69] Li H Zoka Y Sasaki H. Yorino N, Koeda K. A new continuation power flow base on q-limit points. In *47th IEEE International Midwest Symposium on Circuits and Systems*, 2004.

[70] B. Lee, H. Song, S. H. Kwon, G. Jang, J. H. Kim, and V. A. Ajjarapu. A study on determination of interface flow limits in the KEPCO system using modified continuation power flow (MCPF). *IEEE Transactions on Power Systems*, 17:557–564, 2002.

[71] I. Dobson, B. A. Carreras, V. E. Lynch, and D. E. Newman. Complex systems analysis of series of blackouts: cascading failure, critical points, and self-organization. *Chaos*, 17, 2007.

[72] C. DeMarco and A. Bergen. A security measure for random load disturbances in nonlinear power system models. *Circuits and Systems, IEEE Transactions on*, 34(12):1546–1557, Dec 1987.

[73] C. O. Nwankpa, S. M. Shahidehpour, Z. Schuss. A Stochastic Approach to Small Disturbance Stability Analysis. *Transactions on Power Systems*, 7:1519–1528, 1992.

[74] I. Dobson. Computing a closest bifurcation in multidimensional parameter space. *J. Nonlinear Sci.*, 3:307–327, 1993.

[75] M. I. Friswell. Calculation of second and higher order eigenvector derivatives. *Journal of Guidance, Control, and Dynamics*, 18(4):919–921, 1994.

[76] K. Alvehag. *Risk-based methods for reliability investments in electric power distribution systems*. PhD thesis, KTH, May 2011.

[77] J. Condren, T. W. Gedra, and P. Damrongkulkamjorn. Optimal power flow with expected security costs. *IEEE Transactions on Power Systems*, 21(2):541–547, 2006.

[78] Y. V. Makarov, P. Du, S. Lu, T. B. Nguyen, X. Guo, J. W. Burns, and J. F. Gronquist. Wide area security region final report. Technical report, Pacific Northwest National Laboratory, Richland, WA, 2010.

[79] B. Øksendal and A. Sulem. Optimal stochastic impulse control with delayed reaction. *Appl. Math. Optim.*, 58:243–255, 2008.

[80] J. Yong and X. Y. Zhou. *Stochastic Controls: Hamiltonian Systems and HJB Equations*. Springer, 1999.

[81] G. Peskir and A. Shiryayev. *Optimal stopping and free-boundary problems*. Birkhäuser, Basel, Switzerland, 2006.

[82] F. A. Longstaff and E. S. Schwartz. Valuing American options by simulation: A simple least-squares approach. *Review Finan. Stud.*, 14:113–148, 2001.

[83] J. N. Tsitsiklis and B. Van Roy. Optimal stopping of Markov processes: Hilbert space theory, approximation algorithms, and an application to pricing high-dimensional financial derivatives. *IEEE Trans. Automat. Contr.*, 44(10):1840–1851, 1999.

[84] J. N. Tsitsiklis and B. Van Roy. Regression methods for pricing complex American-style options. *IEEE Trans. Neural Netw.*, 12(4):694–703, 2001.

[85] M. J. Brennan and E. S. Schwartz. Evaluating natural resource investments. *J. Bus.*, 58:135–157, 1985.

[86] A. K. Dixit and R. S. Pindyck. *Investment Under Uncertainty*. Princeton University Press, Princeton NJ, 1994.

[87] B. Øksendal and A. Sulem. *Applied stochastic control of jump diffusions*. Springer, Berlin, second edition, 2007.

[88] J.P. Lepeltier and B. Marchal. Théorie générale du contrôle impulsionnel markovien. *SIAM J. Control Optim.*, 22(4):645–665, 1984.

[89] R. Carmona and M. Ludkovski. Pricing asset scheduling flexibility using optimal switching. *Appl. Math. Finance*, 15:405–447, 2008.

[90] B. Djehiche, S. Hamadene, and A. Popier. A finite horizon optimal multiple switching problem. *SIAM J. Control Optim.*, 47(4):2751–2770, 2009.

[91] B. El Asri and S. Hamadéne. The finite horizon optimal multi-modes switching problem: The viscosity solution approach. *Appl. Math. Optim.*, 60:213–235, 2009.

[92] A. Bar-Ilan, A. Sulem, and A. Zanello. Time-to-build and capacity choice. *Journal of Economic Dynamics and Control*, 26(1):69 – 98, 2002.

[93] H. Latorre. *Modeling and Control of VSC-HVDC Transmissions*. PhD thesis, KTH, 2011.

[94] R. Eriksson. *Coordinated control of HVDC links in transmission systems*. PhD thesis, KTH, 2011.

[95] Alberta Electric System Operator. Wind power / AIL data (*http://www.aeso.ca/gridoperations/20544.html*), May 2011.

[96] J. Ma and J. Yong. *Forward-backward stochastic differential equations and their applications*. Springer, Berlin Heidelberg, 2007.

[97] Z. Wu and F. Zhang. Stochastic maximum principle for optimal control problems of forward-backward systems involving impulse controls. *IEEE Transactions on automatic control*, 56(6):1401–1406, 2011.

[98] S. Peng and Z. Yang. Anticipated backward stochastic differential equations. *The Annals of Probability*, 37(3):877–902, 2009.